

EUROPEAN ORGANISATION FOR NUCLEAR RESEARCH (CERN)



JHEP 03 (2017) 157
DOI: [doi:10.1007/JHEP03\(2017\)157](https://doi.org/10.1007/JHEP03(2017)157)



CERN-EP-2016-28
11th May 2017

Measurement of charged-particle distributions sensitive to the underlying event in $\sqrt{s} = 13\text{ TeV}$ proton–proton collisions with the ATLAS detector at the LHC

The ATLAS Collaboration

We present charged-particle distributions sensitive to the underlying event, measured by the ATLAS detector in proton–proton collisions at a centre-of-mass energy of 13 TeV, in low-luminosity Large Hadron Collider fills corresponding to an integrated luminosity of 1.6 nb^{-1} . The distributions were constructed using charged particles with absolute pseudorapidity less than 2.5 and with transverse momentum greater than 500 MeV, in events with at least one such charged particle with transverse momentum above 1 GeV. These distributions characterise the angular distribution of energy and particle flows with respect to the charged particle with highest transverse momentum, as a function of both that momentum and of charged-particle multiplicity. The results have been corrected for detector effects and are compared to the predictions of various Monte Carlo event generators, experimentally establishing the level of underlying-event activity at LHC Run 2 energies and providing inputs for the development of event generator modelling. The current models in use for UE modelling typically describe this data to 5% accuracy, compared with data uncertainties of less than 1%.

1 Introduction

To perform precise Standard Model measurements or to search for new physics phenomena at hadron colliders, it is important to have a good understanding not only of the primary short-distance hard scattering process, but also of the accompanying interactions of the rest of the proton–proton collision – collectively termed the underlying event (UE). As the UE is an intrinsic part of the same proton–proton collision as any “signal” partonic interaction, accurate description of its properties by Monte Carlo (MC) event generators is important for the LHC physics programme.

In modelling terms, the UE can receive contributions from initial- and final-state radiation (ISR, FSR), from the QCD evolution of colour connections between the hard scattering and the beam-proton remnants, and from additional hard scatters in the same p - p collision, termed multiple partonic interactions (MPI). As it is significantly influenced by physics not currently calculable from first principles, the measurement of the UE’s properties is crucial not only for better understanding of the mechanisms involved but also to provide input for empirical tuning of the free parameters of phenomenological UE models in MC event generators.

It is impossible to uniquely separate the UE from the hard scattering process on an event-by-event basis, but observables can be defined which are particularly sensitive to the properties of the UE. Measurements of such observables have been performed in p p collisions between $\sqrt{s} = 900\text{ GeV}$ and 7 TeV in ATLAS [1–5], ALICE [6] and CMS [7–9]. UE observables were also previously measured in $p\bar{p}$ collisions in dijet and Drell–Yan events at CDF, with centre-of-mass energies of $\sqrt{s} = 1.8\text{ TeV}$ [10, 11] and 1.96 TeV [12].

In this paper we report the measurement of UE observables with the ATLAS detector [13] at the LHC, using charged particles in 1.6 nb^{-1} of proton–proton collisions at a centre-of-mass energy of 13 TeV .

2 Underlying-event observables

The UE observables in this study are constructed from “primary” charged particles in the pseudorapidity range $|\eta| < 2.5$,¹ whose transverse momentum (p_T) is required to be greater than 500 MeV . Primary charged particles are defined as those with a mean lifetime $\tau > 300\text{ ps}$, which are either directly produced in p p interactions or from subsequent decays of particles with a lifetime $\tau < 30\text{ ps}$. This measurement follows the fiducial particle definition used in the ATLAS 13 TeV minimum-bias measurement [14] excluding particle species with τ in the range 30 to 300 ps and their decay products. The charged particles falling in this range are strange baryons with a very low reconstruction probability, whose decays are inconsistently modelled in MC generators. Their exclusion from the fiducial acceptance definition hence avoids the need to apply large and poorly defined corrections to particle level for these species, making the measurement more accurate.

This measurement uses the established form of UE observables [1–7, 9, 10, 12], in which the azimuthal plane of the event is segmented into several distinct regions with differing sensitivities to the UE. As

¹ ATLAS uses a right-handed coordinate system with its origin at the nominal interaction point (IP) in the centre of the detector and the z -axis along the beam pipe. The x -axis points from the IP to the centre of the LHC ring, and the y -axis points upward. Cylindrical coordinates (r, ϕ) are used in the transverse plane, ϕ being the azimuthal angle around the beam pipe. The pseudorapidity is defined in terms of the polar angle θ as $\eta = -\ln \tan(\theta/2)$.

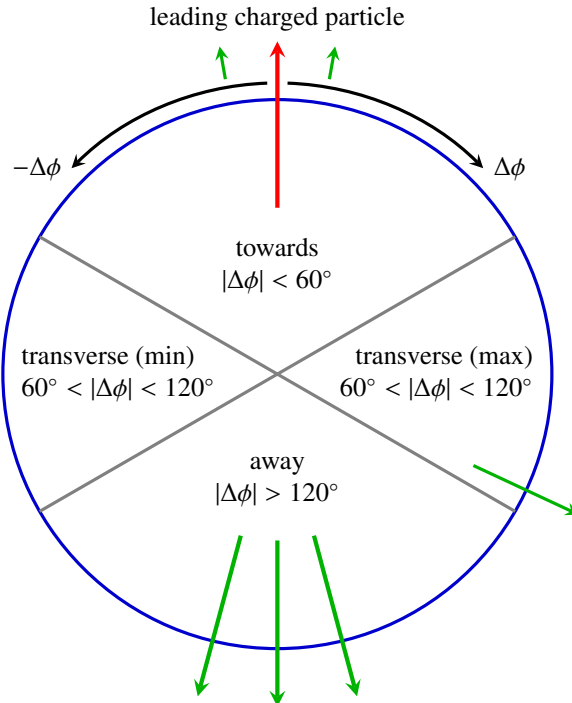


Figure 1: Definition of regions in the azimuthal angle with respect to the leading (highest- p_T) charged particle, with arrows representing particles associated with the hard scattering process and the leading charged particle highlighted in red. Conceptually, the presence of a hard-scatter particle on the right-hand side of the transverse region, increasing its $\sum p_T$, typically leads to that side being identified as the “trans-max” and hence the left-hand side as the “trans-min”, with maximum sensitivity to the UE.

illustrated in Figure 1, the azimuthal angular difference with respect to the leading (highest- p_T) charged particle, $|\Delta\phi| = |\phi - \phi_{\text{lead}}|$, is used to define the regions:

- $|\Delta\phi| < 60^\circ$, the “towards region”;
- $60^\circ < |\Delta\phi| < 120^\circ$, the “transverse region”; and
- $|\Delta\phi| > 120^\circ$, the “away region”.

As the scale of the hard scattering increases, the leading charged particle acts as a convenient indicator of the main flow of hard-process energy. The towards and away regions are dominated by particle production from the hard process and are hence relatively insensitive to the softer UE. In contrast, the transverse region is more sensitive to the UE, and observables defined inside it are the primary focus of UE measurements.

A further refinement is to distinguish on a per-event basis between the more and the less active sides of the transverse region [15, 16], defined in terms of their relative scalar sums of primary charged-particle p_T and termed “trans-max” and “trans-min” respectively. The trans-min region is relatively insensitive to wide-angle emissions from the hard process, and the difference between trans-max and trans-min observables (termed the “trans-diff”) hence represents the effects of hard-process contamination. In this analysis, an event must have a non-zero primary charged-particle multiplicity in the trans-min region in order to be included in either the trans-min, -max, or -diff observables.

Table 1: Definitions of the measured observables in terms of primary charged particles. The upper group of observables are used to define the x -axes of the plots to be shown in Section 8, and the lower group are the mean values of distributions constructed in each x -bin and plotted on the y -axes. The $\delta\eta\delta\phi$ scale factors convert the raw measurements of regional N_{ch} and $\sum p_{\text{T}}$ into densities per unit $\eta-\phi$ and their values change depending on the region/bin-sizes being considered, so that the density variables are everywhere directly comparable.

Symbol	Description
BINNED VARIABLES	
$p_{\text{T}}^{\text{lead}}$	Transverse momentum of the leading charged particle
$N_{\text{ch}}(\text{transverse})$	Number of charged particles in the transverse region
$ \Delta\phi $	Absolute difference in particle azimuthal angle from the leading charged particle
AVERAGED VARIABLES	
$\langle N_{\text{ch}}/\delta\eta\delta\phi \rangle$	Mean number of charged particles per unit $\eta-\phi$ (in radians)
$\langle \sum p_{\text{T}}/\delta\eta\delta\phi \rangle$	Mean scalar p_{T} sum of charged particles per unit $\eta-\phi$ (in radians)
$\langle \text{mean } p_{\text{T}} \rangle$	Mean per-event average p_{T} of charged particles (≥ 1 charged particle required)

The variables measured in this analysis, constructed using charged particles with $p_{\text{T}} > 0.5 \text{ GeV}$ and $|\eta| < 2.5$, with a higher- p_{T} requirement of $p_{\text{T}}^{\text{lead}} > 1 \text{ GeV}$ placed on the leading charged particle, are described in Table 1. These variables are divided into two groups: first the “binned” per-event or per-particle quantities used to define the horizontal axes in the unfolded observables of Section 8; and secondly the “averaged” mean values of distributions of per-event quantities to be studied as functions of the binned variables – a construction known as a “profile”. The second-group variables are defined for each bin and (except for $\langle \text{mean } p_{\text{T}} \rangle$, in which the $\eta-\phi$ area factors cancel) are scaled by the corresponding $\delta\eta\delta\phi$ areas to give densities comparable between all such measurements, including between various experiments and collider energies. The area factor $\delta\phi$ is $2\pi/3$ for the toward, transverse & away regions, whereas it is $\pi/3$ for the single-sided trans-min & trans-max regions, and $2\pi/n_{\text{bins}}$ for each of the n_{bins} equally sized bins in distributions plotted against $|\Delta\phi|$. Due to the $|\eta| < 2.5$ fiducial acceptance and the η -independence of the region definitions, $\delta\eta = 5$ in all cases. The profile observables are implemented as profile histograms, presenting the mean values of the “averaged” variables as measured in each bin of another observable. These hence measure the degree of correlation between two event features, either between the UE and hard scattering, or between different UE aspects. The mean charged-particle momentum $\langle p_{\text{T}} \rangle$ is constructed on an event-by-event basis and then averaged over all events to give $\langle \text{mean } p_{\text{T}} \rangle$.

The majority of underlying-event observables study the dependences of the averaged quantities on the transverse momentum of the leading object – here the leading charged particle. The development of this from low to high p_{T} corresponds to the smooth transition from “minimum bias” interactions to the hard-scattering regime focused on by most LHC analyses, and the correlation distributions characterise how soft QCD effects co-evolve with the hard process through this transition. This analysis also studies the dependence of the observables on the azimuthal angle with respect to the leading particle and each region’s charged-particle multiplicity. For the observables studied as a function of relative azimuthal angle, the leading particle is excluded from the spectrum.

3 Monte Carlo modelling of the underlying event

As a physics process related to the bulk structure of protons and not calculable from first-principles perturbative QCD, the underlying event is modelled in Monte Carlo event generator programs by various phenomenological approaches. The scattering subprocess type which contributes most to UE observables is non-diffractive inelastic scattering. In event generator implementations, model-specific choices are made to regulate these processes’ QCD divergences at low scales. In this analysis the observable definitions restrict the effect of diffractive scattering, i.e. colour-singlet exchange, to play a minor role: the $\langle p_T \rangle$ profile observables have been found to be completely insensitive to diffraction, while the N_{ch} and $\sum p_T$ profiles exhibit a 2% effect at low p_T^{lead} and the whole of the N_{ch} vs. $\Delta\phi$ distribution is affected by diffraction at a 1–2% level.

This section reviews relevant features of the PYTHIA 8 [17, 18], HERWIG 7 [19] and EPOS [20, 21] MC event generator models, which are used in this study either for data correction or for comparison to the final corrected data distributions. A summary of the Monte Carlo generator configurations used is given in Table 2.

PYTHIA 8.18/8.21: The PYTHIA generator family is very widely used at the LHC and elsewhere for event modelling, and PYTHIA 8 is its most recent release series. Its key features are leading-logarithmic initial- and final-state parton showers and a Lund string hadronisation model, in addition to particle decays and soft-QCD modelling. Hard-process calculations are performed either via an internal set of leading-order matrix elements, or by reading externally generated hard scattering events.

The PYTHIA 8 approach to soft-QCD modelling uses a parameterised total pp cross-section, which is split into elastic, diffractive, and non-diffractive (ND) inelastic scattering subprocesses. The first two of these again have parameterised cross-sections, and the hadronic ND inelastic cross-section is set by subtracting their contributions from the total.

The ND contribution is modelled using perturbative $2 \rightarrow 2$ QCD matrix elements, dominated by t -channel gluon exchange. As the partonic cross-section for this exceeds the hadronic ND cross-section at low p_T , the existence of MPI is implied and may be used to regularise the cross-section growth. PYTHIA 8 uses an evolved form of the Sjöstrand–van Zijl MPI model [22] in which the eikonal formalism is applied to give a model with a Poisson distribution of multiple perturbative scatterings whose mean rate depends on the scale of the hard process (interpreted as the reciprocal of the pp impact parameter), the proton form factor, and the ratio of hadronic to partonic ND cross-sections. An ansatz is used to regularise cross-section growth at low p_T , with a weak power-law evolution of the regularisation parameter with \sqrt{s} . The current form of the model also interleaves MPI emissions with parton shower evolution, allows several forms of matter overlap parameterisation, and interacts with a non-perturbative annealing procedure for reconfiguration of colour strings during hadronisation (the “colour reconnection” mechanism).

As MPI and hadronisation modelling are phenomenological and even the perturbative parton shower formalism has some configurational freedom, many parameter optimisations (“tunes”) of PYTHIA 8 have been performed. The following are considered in this study:

- ATLAS’s dedicated underlying-event tune is “A14” [23]. Its configuration is based on the NNPDF2.3 LO [24] parton density function (PDF), and was optimised for the description of several underlying event and jet radiation observables, including jet, Drell–Yan, and $t\bar{t}$ data, with an emphasis on high-scale events.

Table 2: Details of the MC models used. Some tunes are focused on describing the minimum-bias (MB) distributions better, while the rest are tuned to describe underlying event (UE) or double parton scattering (DPS) distributions.

Generator	Version	Tune	PDF	Focus	From
PYTHIA 8	8.185	A2	MSTW2008 LO	MB	ATLAS
PYTHIA 8	8.185	A14	NNPDF2.3 LO	UE	ATLAS
PYTHIA 8	8.186	Monash	NNPDF2.3 LO	MB/UE	Authors
HERWIG 7	7.0.1	UE-MMHT	MMHT2014 LO	UE/DPS	Authors
EPOS	3.4	LHC	—	MB	Authors

- An alternative tune, “Monash” [25], is used for comparison. Like A14, it was constructed using Drell–Yan and underlying-event data from ATLAS, but also data from CMS, from the SPS, and from the Tevatron in order to constrain energy scaling. It also uses the NNPDF 2.3 LO PDF, and has more of a general-purpose / low- p_T emphasis than A14. This tune gives an excellent description of the ATLAS 7, 8 and 13 TeV minimum-bias p_T spectra [14, 26, 27].
- The ATLAS minimum-bias tune “A2” [28] was used for deriving detector corrections. This is based on the MSTW2008 LO PDF [29], and was tuned using ATLAS minimum-bias data at 7 TeV for the MPI parameters, in addition to the older PYTHIA 8 tune “4C” values for fragmentation parameters. It provides a good description of minimum-bias and transverse energy flow data [30].

The PYTHIA 8 predictions shown in this paper use large MC samples from versions 8.185 and 8.186, but checks against the newer 8.2xx release series (specifically, version 8.210) found no distinguishable difference.

HERWIG 7.0.1: The HERWIG family of MC generators has also been heavily used in many collider physics studies, and HERWIG 7 is the most recent major series [19, 31]. Like PYTHIA, it is a fully exclusive hadron-level generator, containing leading-logarithmic parton showers, hadronisation and decays, an MPI mechanism, and capabilities for parton-shower matching to higher-order hard processes. It uses a cluster hadronisation scheme, and angular-ordered and dipole parton showers.

The soft-QCD modelling in HERWIG 7 (and HERWIG++ before it) uses an eikonal model similar to PYTHIA’s, but with some distinctions. The same treatment with Poisson-distributed simulation of many independent perturbative QCD scatters is then used, but with a simpler MPI parameterisation than in PYTHIA: the functional form of the proton electromagnetic form factor is used to parameterise the hadronic matter distribution rather than PYTHIA’s very flexible parameterisation, and a continuation of eikonal scattering down to very low p_T values is applied in place of PYTHIA’s phenomenological regularisation of eikonal scattering below the p_T cutoff. The HERWIG soft eikonal scattering model uses distinct matter distributions for soft and hard MPI scattering, and introduces a \sqrt{s} -dependence of MPI parameters similar to that found in PYTHIA. The parameters of this model are highly constrained by fits to total cross-section and elastic scattering data [31, 32]. A colour-disruption mechanism is used in hadronisation, as a cluster-oriented analogy to the PYTHIA colour reconnection, to improve the quality of minimum-bias observable description.

The HERWIG 7 default tune, H7-UE-MMHT with the MMHT2014 LO PDF [33], has been used. This tune, like its HERWIG++ predecessors, is based on LHC and Tevatron underlying-event meas-

urements, as well as double parton scattering data [34]. It provides a good description of all these observables for \sqrt{s} from Tevatron 300 GeV to LHC 7 TeV.

EPOS 3.4: An alternative approach is taken by Epos, a specialist soft-QCD/cosmic-ray air-shower MC generator based on an implementation of parton-based Gribov–Regge theory [20]. This is a QCD-inspired effective-field theory describing the hard and soft scattering simultaneously. It incorporates elements of collective flow modelling from nuclear and heavy-ion physics, using hydrodynamic flow modelling in high-density regions and a string-based hadronisation model elsewhere. As a result the Epos calculations do not make use of standard parton density functions. Using this version, equivalent to the so-called “LHC tune” of version 1.99 [21], Epos gives a very good description of ATLAS’s 13 TeV minimum-bias data, including the tails of distributions where UE physics should be involved, but as it lacks a dedicated hard scattering component it is unclear how accurate its description of UE correlations can be.

Detector-level simulation

The PYTHIA 8 A2 sample and an MC simulation of single particles distributed to populate the high- p_T region were used to derive the detector corrections for these measurements. Smaller samples produced with the Epos generator were used to cross-check the validity of the correction procedure.

These events were processed through the ATLAS detector simulation framework [35], which is based on GEANT 4 [36]. They were then reconstructed and analysed using the same processing chain as for data. In all Monte Carlo samples the distribution of the primary vertex position was reweighted to match the distribution in data.

4 The ATLAS detector

The ATLAS detector is described in detail in Ref. [13]. In this analysis, the trigger system and inner tracking detectors are of particular relevance.

The inner tracking detector is immersed in the 2 T axial magnetic field of a superconducting solenoid, and measures the trajectories of charged particles in the pseudorapidity range $|\eta| < 2.5$ with full azimuthal coverage. It consists of a silicon pixel detector (pixel), a silicon microstrip detector (SCT) and a straw-tube transition radiation tracker (TRT), split into a barrel and two endcap components. The barrel consists of 4 pixel layers, 4 layers of SCT modules with back-to-back silicon strip sensors, and 73 layers of TRT straws; each endcap has 3 pixel layers, 9 SCT layers, and 160 TRT straw layers. The pixel, SCT and TRT have $r-\phi$ position resolutions of 10 μm , 17 μm , and 130 μm respectively, and the pixel (apart from the innermost barrel layer) and SCT have resolutions of 115 μm and 580 μm respectively in the z -direction for the barrel modules and in the r -direction for the endcaps.

The innermost pixel layer, the “insertable B-layer” (IBL), was added between LHC Runs 1 and 2, around a new narrower (radius of 25 mm) and thinner beam pipe [37]. It is composed of 14 lightweight staves arranged in a cylindrical geometry, each made of 12 silicon planar sensors in its central region and 2 \times 4 three-dimensional sensors at the ends. The IBL pixel dimensions are 50 \times 250 μm in the ϕ and z directions (compared with 50 \times 400 μm for other pixel layers). The smaller radius and the reduced pixel size result in improvements of both the transverse and longitudinal impact parameter resolutions. In addition, the

services for the existing pixel detector were upgraded, significantly reducing the material in $|\eta| > 1.5$, in particular at the boundaries of the active tracking volume. A track from a charged particle traversing the barrel detector typically has 12 silicon measurement points (hits), of which 4 are pixel and 8 are SCT, and more than 30 TRT straw hits.

The ATLAS detector has a two-level trigger system: level 1 and the high-level trigger [38]. Events used in this analysis were required to satisfy level-1 triggers using the minimum-bias trigger scintillators (MBTS). These are mounted at each end of the detector in front of the liquid-argon endcap-calorimeter cryostats at $z = \pm 3.56$ m and are segmented into two rings in pseudorapidity ($2.07 < |\eta| < 2.76$ and $2.76 < |\eta| < 3.86$), with 8 azimuthal sectors in the inner ring and 4 in the outer. The MBTS scintillator was replaced for Run 2 due to radiation damage incurred in Run 1. The MBTS triggers fired if at least one MBTS hit from either side of the detector was recorded above threshold.

5 Event and object selection

This measurement uses data taken in a special configuration of the LHC, with low beam currents and reduced beam focusing, producing a low mean number of interactions per bunch-crossing, $\langle\mu\rangle$, between 0.003 and 0.03. This configuration and event selection were earlier used and documented in detail in the ATLAS 13 TeV minimum-bias analysis [14], and so only a summary is given here.

Trigger: Events were selected from colliding proton bunches using a trigger which required one or more MBTS counters above threshold on either side of the detector. The efficiency of this trigger was measured to be 99% for low-multiplicity events and to rapidly rise to 100% for events with higher track multiplicities. The trigger requirement does not bias the p_T and η distributions of selected tracks in this analysis due to the $p_T^{\text{lead}} > 1$ GeV requirement.

Primary vertex: Each event was required to contain a primary vertex reconstructed from at least two tracks with $p_T > 100$ MeV and selection requirements specific to vertexing [39]. The canonical primary vertex was identified as that with the highest $\sum p_T^2$ of its associated tracks. To reduce contamination from events with more than one interaction in a bunch crossing (“pile-up”), events containing more than one primary vertex with four or more associated tracks were removed. The contributions from non-collision backgrounds and events where two interactions are reconstructed as a single vertex were studied in data and found to be negligible.

A total of 66 million data events passed the trigger and vertex selection requirements for this analysis.

Tracks: Tracks were reconstructed starting from hits in the silicon detectors and then extrapolated to include information from the TRT. Each track required hits in both the pixel system and the SCT, including a requirement of a hit in the innermost expected pixel layer to reject secondary particles.

All tracks were reconstructed within the geometric acceptance of the inner detector, $|\eta| < 2.5$. In this analysis, all selected tracks were additionally required to have a transverse momentum above 500 MeV, and both the transverse impact parameter and the projected longitudinal impact parameter with respect to the primary vertex were required to be less than 1.5 mm. For high- p_T tracks, a further requirement was placed on the χ^2 probability of the track fit, to suppress mismeasured tracks. The selected events were additionally required to contain at least one track with a transverse momentum above 1 GeV.

Backgrounds: The contributions from non-collision background events, events with more than one interaction, and fake tracks (those formed by a random combination of hits or from a combination of hits from several particles) were found to be negligible. The contribution from secondary particles was estimated as in Ref. [14].

6 Correction to particle level

In order to compare the measured underlying-event distributions with model predictions in the particle-level fiducial phase space, the observables have been corrected for detector effects. These corrections include explicit accounting for inefficiencies due to the trigger selection, vertexing, and track reconstruction, by weighting the events and tracks by inverse efficiencies. A further correction has been applied to account for non-linear effects, particularly azimuthal re-orientation of the event which occurs should the leading charged particle not be reconstructed. In this situation the identification of the towards, transverse, and away regions can differ from that at particle level, leading to “wrong” track–region associations. Re-orientation mainly affects events with a low number of charged particles, and has been corrected using a dedicated method. The track-weight correction is described first, followed by the method to account for event re-orientation.

6.1 Event and track weighting

The weighting procedure for correcting measured distributions to particle level is affected by the primary vertex reconstruction efficiency, the tracking efficiency, the rate of non-primary particles, and the rate of charged strange baryons. Before defining the weights, we summarise these aspects of the vertexing and tracking performance:

Vertexing efficiency: The vertex reconstruction efficiency, ϵ_{vtx} , was determined from data by taking the ratio of the number of selected events with a reconstructed vertex to the total number of events with the requirement of a primary vertex removed. The efficiency was close to 100% except for events in which exactly one $p_T > 500$ MeV analysis track was found in the inner detector – for these the vertexing efficiency was found to be 90%. Since the leading-track $p_T > 1$ GeV requirement in the analysis is correlated with higher track multiplicities, the effect of the vertex reconstruction on the analysis is small.

Tracking efficiency: The efficiency to reconstruct primary charged particles was determined from simulation by matching MC-generator primary charged particles to tracks reconstructed from simulated inner-detector hits. For particles at the analysis transverse-momentum cutoff of $p_T = 500$ MeV, the track reconstruction is $\sim 85\%$ efficient for central pseudorapidity, and decreases to 65% for $|\eta| \sim 2.5$ at the edge of the inner tracking detector; these efficiencies are higher for tracks with higher p_T , for example 90% and 80% respectively for $p_T = 10$ GeV.

Most of the loss in tracking efficiency is due to particle interactions with the detector material and support structures, and hence a good description of the detector material is needed. The ATLAS inner tracker upgrades for LHC Run 2 necessitated a new study of the detector material uncertainties, which are detailed in Ref. [14]. The track reconstruction efficiency for $|\eta| > 1.5$ is corrected using a method that compares the efficiency to extend a track reconstructed in the pixel detector into the SCT in data and simulation.

Rate of non-primary tracks: There are several sources of non-primary tracks: 1) tracks from hadronic interaction of particles with the detector material, 2) decay products from particles with strange quark content, mostly K^0 and Λ^0 decays, 3) photon conversions. The last of these is negligible for the tracks with $p_T > 500$ MeV used in this analysis. The rate of non-primary tracks was determined by comparing side-band fits of MC simulation impact parameter distributions to the data, leading to an estimated 2.3% of non-primary tracks in data for the $p_T > 500$ MeV track selection, and a smaller effect for higher- p_T tracks.

Fraction of charged strange baryons: Charged strange baryons and their decay products have low reconstruction efficiency, unless they have large transverse momentum. With the fiducial primary particle definition used here, the fraction of tracks due to strange baryons with $p_T = 10$ GeV is 1%, while it is much smaller than 1% at lower p_T . With our fiducial primary particle definition, tracks originating from charged strange baryons are classified as a background. An estimate of their contribution was made using the Epos generator, a choice motivated both by Epos providing the best current description of charged strange baryon rates as measured by the ALICE experiment [40], and by substantial variation of strange baryon modelling between different MC generators.

Weighting: The effect of events lost due to the trigger and vertex requirements was corrected by an event-by-event weight,

$$w_{\text{ev}}(n_{\text{sel}}^{\text{BL}}, \eta) = \frac{1}{\epsilon_{\text{trig}}(n_{\text{sel}}^{\text{BL}})} \cdot \frac{1}{\epsilon_{\text{vtx}}(n_{\text{sel}}^{\text{BL}}, \eta)}, \quad (1)$$

where ϵ_{trig} is the trigger efficiency and $n_{\text{sel}}^{\text{BL}}$ is the multiplicity of “beam line” selected tracks, which have the same selection requirements as analysis tracks except that no vertexing requirement is applied and hence there is no restriction on the longitudinal impact parameter.

To correct for inefficiencies in the track reconstruction, the distributions of the selected analysis tracks were corrected with track-by-track weights,

$$w_{\text{trk}}(p_T, \eta) = \frac{1}{\epsilon_{\text{trk}}(p_T, \eta)} \cdot (1 - f_{\text{nonp}}(p_T, \eta) - f_{\text{okr}}(p_T, \eta) - f_{\text{sb}}(p_T)), \quad (2)$$

where ϵ_{trk} is the tracking efficiency, and f_{nonp} , f_{okr} and f_{sb} are respectively the fractions of non-primary tracks, of out-of-kinematic-range tracks (i.e. tracks mis-reconstructed as within the fiducial p_T and η acceptances, but which actually originated from outside those ranges), and of weakly decaying charged strange baryons.

This track weight was used in the construction of the N_{ch} , $\sum p_T$, and $\Delta\phi$ distributions, and the mean p_T in the event, determined using the weighted average $\langle p_T \rangle = \sum_{i \in \text{tracks}} p_T^i w_{\text{trk}}^i / \sum_{i \in \text{tracks}} w_{\text{trk}}^i$.

For the distributions binned in charged multiplicity, this weight was not used to correct the binning variable, since this induces migrations subject to fluctuations not accounted for by track weighting. This correction was instead handled by the residual correction method described in the next section.

6.2 Re-orientation correction

The re-orientation correction was based on the HBOM method [41], in which the effect of the detector and reconstruction algorithms on an observable (i.e. a histogram bin value) is treated as an operator A . The observed reconstruction-level value of an observable, X^{obs} , is hence related to its true value X^{true} as

$X^{\text{obs}} = AX^{\text{true}}$, but one can continue to apply A to the modified event, so that the k th additional application gives $X_k^{\text{obs}} = A^k X^{\text{obs}} = A^{k+1} X^{\text{true}}$. If the evolution of the observable’s value is a smoothly varying function under such iterations, an n^{th} -order polynomial function $P_n(k)$ can be fitted to X_k^{obs} for $k \geq 0$, and then extrapolated back to $k = -1$, i.e. X^{true} . This procedure is carried out independently for each bin of each distribution. It is distinct from the unfolding approach used in Refs. [4] and [14], chosen because it is fully data-driven, i.e. does not rely on simulation performance or require reweighting of MC events to data.

In this analysis, A encodes the effects of track reconstruction, i.e. each application of A in principle smears the track kinematics and considers the possibility that some tracks would not have been reconstructed – directly inducing re-orientation should the leading track experience such a fate. These effects are described by the measured tracking resolutions and efficiencies, as functions of track η and p_T , but the efficiency was found to dominate and the resolution to be negligible, so A reduces to random discarding of tracks according to their reconstruction efficiency. For the profile distributions, a weight proportional to the inverse of tracking efficiency (as above) was applied in each HBOM iteration step, k , to make the effect on the observable less dramatic and more easily parameterisable.

To avoid correlations between observables with different k values, each X_k^{obs} was calculated independently, using a distinct random seed and k iterations of track discarding starting from the set of reconstructed ($k = 0$) tracks. Second-order polynomials and a maximum of $k = 4$ HBOM iterations were used as the nominal configuration, with variations being used to derive an extra systematic uncertainty, described in the following section.

7 Systematic uncertainties

Several categories of systematic uncertainties that may influence the distributions after corrections and unfolding were quantified, and their magnitudes are summarised in Table 3. The sources of uncertainty and the methods used to estimate them were the following:

Trigger and vertexing: The systematic uncertainties were found to be negligible.

Track reconstruction: The uncertainties in track reconstruction efficiency principally arise from imperfect knowledge of the material in the inner detector. The new insertable B-layer and changes to pixel detector services in the $|\eta| > 1.5$ region add uncertainties not included in the inner-detector material assessments performed during Run 1: these have been evaluated by comparison of data to simulation, and by comparisons of simulations with different compositions of interacting particles. The result is an estimate of reconstruction efficiency uncertainty between 0.4% and 1.5% [14]. An additional systematic uncertainty arises from possible biases and degradation in the p_T^{lead} measurement: these effects were determined in Ref. [14] and estimated to affect the tail of the p_T^{lead} distribution by 4–5%.

Non-primary particles: The systematic uncertainties were propagated by modification of track weights. The systematic uncertainty on the selected non-primary track fraction was estimated to be 24%, using variations of the fit range in the tail of the impact parameter distributions, and different MC generators and different shape assumptions for the extrapolation of the fraction from the side-bands to the signal region. The MC variation is responsible for the most significant contribution to this uncertainty. The systematic uncertainty due to the fraction of charged strange baryons was derived using the deviations of generator predictions from Epos [14].

Table 3: Summary of systematic uncertainties for each class of UE observable, broken down by origin.

Observable	Range of values			
	Material	Non-primaries	Non-closure	Parameterisation
N_{ch} or $\sum p_T$ vs. $\Delta\phi$	0.9%	0.6%	0–0.6%	0–0.4%
N_{ch} or $\sum p_T$ vs. p_T^{lead}	0.5–1.0%	0.3–0.6%	0–2.5%	0–0.4%
$\langle \text{mean } p_T \rangle$ vs. N_{ch}	0–0.5%	0–0.5%	—	0.5% (combined)
$\langle \text{mean } p_T \rangle$ vs. p_T^{lead}	0–0.4%	0–0.3%	—	0.5% (combined)

Unfolding: The systematic uncertainties associated with the HBOM unfolding have two distinct sources:

Non-closure: The HBOM correction procedure is in principle independent of the Monte Carlo generator modelling. However, the method shows deficiencies in some regions and distributions. The relative size of the observed non-closure (i.e. non-reproduction of a known input) derived using PYTHIA 8 A2 was therefore applied as a correction. The size of the correction is included as a systematic uncertainty, everywhere less than 2.5%. The measured transverse momentum distribution of the leading charged particle was found to be consistent with the result obtained using Bayes-inspired iterative unfolding [42] within the estimated bias.

Parameterisation: The statistical uncertainty of the HBOM method was derived for each bin using Monte Carlo sampling: for each HBOM(k) iteration, samples were drawn from a Gaussian distribution corresponding to the point uncertainty, and 1000 independent replica HBOM fits were performed. The resulting uncertainty contribution is derived from the replicas' central 68% confidence interval. An additional systematic uncertainty, estimating the stability of the fit method, was derived by using different numbers of HBOM iterations k and polynomial degrees n .

For the results presented in the following section, these independent sources of systematic uncertainty have been combined in quadrature to form single representative systematic uncertainty estimates.

8 Results

The unfolded distributions and their main features are discussed here, and in Figures 2, 3, 5 and 6 are compared to model predictions from PYTHIA 8 (the A14, A2 and Monash tunes), HERWIG 7, and EPOS. These model predictions were obtained using the analysis' associated Rivet routine [43].

Leading charged-particle p_T Figure 2 shows the unit-normalised distribution of events with respect to the transverse momentum of the leading charged particle, p_T^{lead} . This is a steeply falling distribution, with a change of slope for $p_T^{\text{lead}} \gtrsim 5$ GeV: a form which is broadly modelled by all generators. The PYTHIA 8 A14 and Monash tunes, as well as Epos, model the distribution within 15% out to $p_T^{\text{lead}} = 30$ GeV, while the PYTHIA 8 A2 minimum-bias tune predicts too hard a spectrum in the high p_T^{lead} tail. HERWIG 7 peaks strongly at the lowest p_T^{lead} and alternates between under- and over-shooting the data at higher scales, finally producing a softer tail than seen in data.

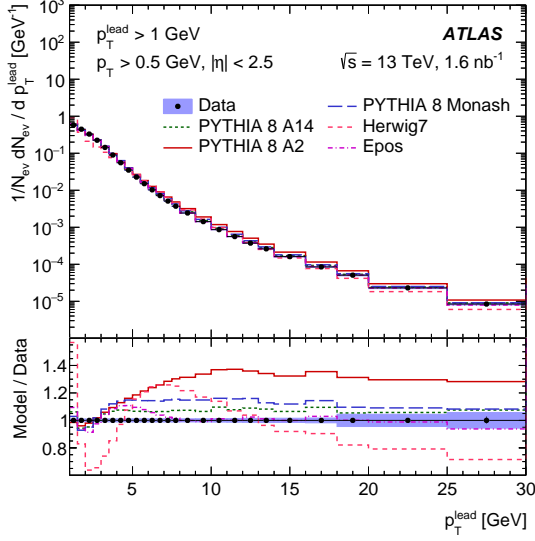


Figure 2: Unit-normalised distribution of the transverse momentum of the leading charged particle, $p_T^{\text{lead}} > 1 \text{ GeV}$, compared to various generator models. The error bars on data points represent statistical uncertainty and the blue band the total combined statistical and systematic uncertainty.

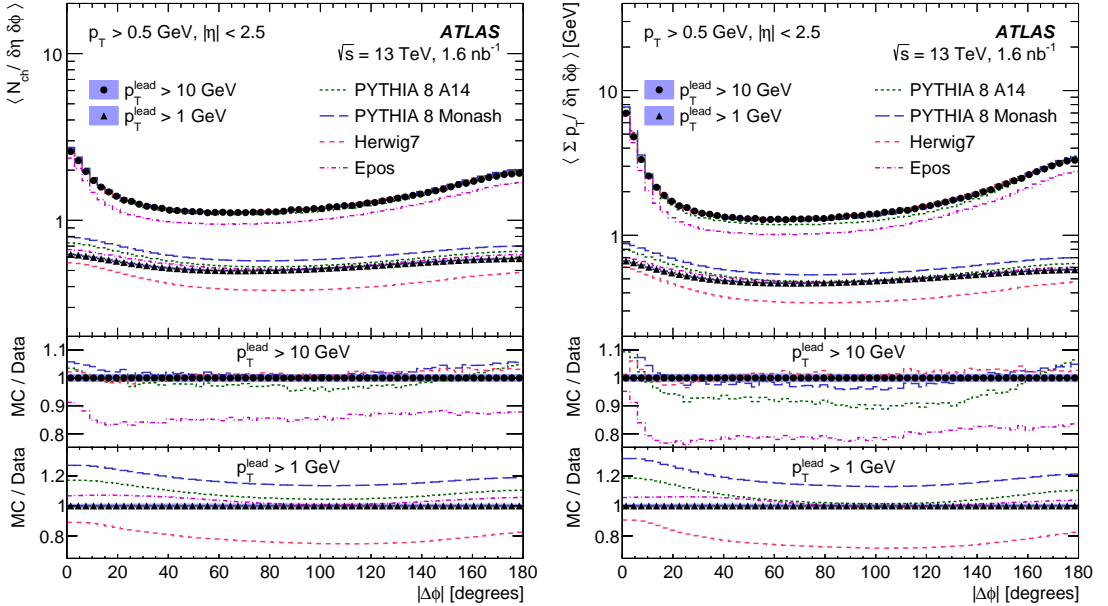


Figure 3: Distributions of mean densities of charged-particle multiplicity N_{ch} (left) and $\sum p_T$ (right) as a function of $|\Delta\phi|$ (with respect to the leading charged particle) for $p_T^{\text{lead}} > 1 \text{ GeV}$ and $p_T^{\text{lead}} > 10 \text{ GeV}$ separately, with comparisons to MC generator models. The error bars on data points represent statistical uncertainty and the blue band the total combined statistical and systematic uncertainty.

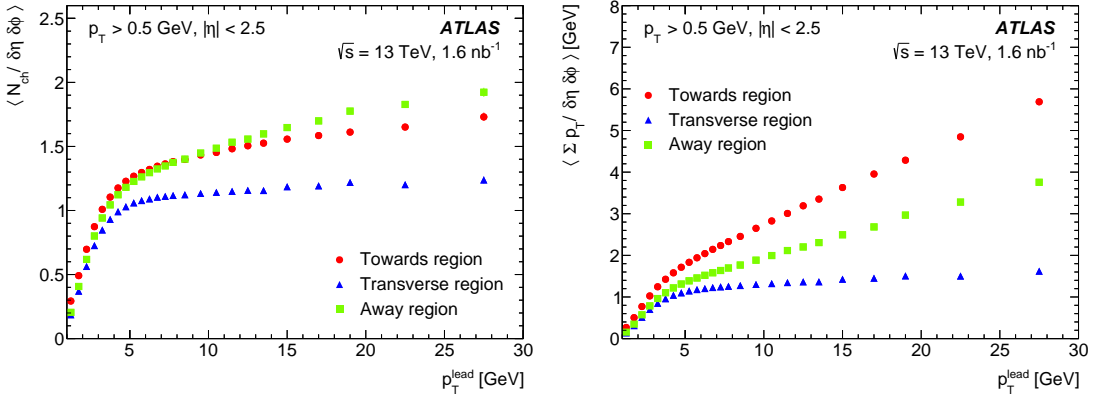


Figure 4: Mean η - ϕ densities of charged-particle multiplicities (left) and $\sum p_T$ (right) as a function of the transverse momentum of the leading charged particle in the transverse, towards, and away azimuthal regions. The error bars, which are mostly hidden by the data markers, represent combined statistical and systematic uncertainty.

Angular distributions versus leading charged particle Figure 3 shows the mean multiplicity and $\sum p_T$ distributions as a function of azimuthal angle with respect to the leading particle for different p_T^{lead} requirements. Two event selections are shown here: the $p_T^{\text{lead}} > 1 \text{ GeV}$ cut common to all observables, and a harder $p_T^{\text{lead}} > 10 \text{ GeV}$ requirement.

The difference between these two selections illustrates the transition from relatively isotropic minimum-bias scattering to the emergence of hard partonic scattering structure and hence a dominant axis of energy flow. This event structure with least activity perpendicular to the leading-object axis, i.e. away from $\Delta\phi = 0$ and 180° , is seen for both selections and both observables but is much stronger for the event subset with the higher $p_T^{\text{lead}} > 10 \text{ GeV}$ requirement: this demonstrates the evolution of event shape as a hard scattering component develops.

There is no clear “best” MC model for these observables. Epos performs best in the more inclusive $p_T^{\text{lead}} > 1 \text{ GeV}$ selection, followed by PYTHIA 8 A14; HERWIG 7 significantly undershoots while PYTHIA 8 Monash is everywhere above the data. But in the hard-scattering $p_T^{\text{lead}} > 10 \text{ GeV}$ event selection, HERWIG 7 and Monash perform best, with a slight undershoot from PYTHIA 8 A14 and a large one from EPOS. These orderings apply to both the N_{ch} and $\sum p_T$ variables, although to different extents.

N_{ch} and $\sum p_T$ densities in transverse/towards/away regions Figure 4 shows the evolution of the mean charged-particle multiplicity and $\sum p_T$ densities with the p_T of the leading charged particle, from 1 to 30 GeV. For both observables, the towards, transverse, and away regions are shown overlaid for ease of comparison.

The primary feature is the general shape seen in all curves: starting close to zero at low p_T^{lead} , there is first a very rapid rise in activity in which the three regions are not strongly distinguished, then an abrupt transition at $p_T^{\text{lead}} \approx 5 \text{ GeV}$ above which the three regions have quite distinct behaviours. The initial rapid rise to a roughly stable value of ~ 1 charged particle or $\sim 1 \text{ GeV}$ per unit η - ϕ area is known as the “pedestal effect”. In modelling terms this reflects a reduction of the pp impact parameter with increasing p_T^{lead} , and hence the transition between the minimum-bias and hard-scattering regimes.

Secondly, the shape of the transverse region is different from the other two in both observables – it almost completely plateaus after $p_T^{\text{lead}} \approx 5 \text{ GeV}$, while the towards and away regions continue to rise nearly

linearly with p_T^{lead} . This characteristic feature of UE profile observables is the empirical demonstration of the azimuthal-region paradigm for UE analysis: the hard process dominates the towards and away regions, which continue to increase in activity as the hard-process scale grows, but the transverse region is relatively unaffected. This is consistent with the pedestal effect where the overlap between colliding protons is complete and hence any further growth is due to connections to, or contaminations from, the hard process rather than more MPI scattering.

An interesting feature is that for $p_T^{\text{lead}} \gtrsim 7 \text{ GeV}$ the *away* region actually becomes the one with highest charged-particle multiplicity, despite not containing the highest- p_T charged particle. By the $\sum p_T$ density measure, however, the towards region is unambiguously the most active region for all p_T^{lead} values.

N_{ch} and $\sum p_T$ densities in trans-min/max/diff regions Figure 5 focuses on the UE-dominated transverse region, and its per-event specialisations trans-min, -max, and -diff. Between these, the trans-min is the most sensitive to MPI effects, i.e. the pedestal, while the trans-max includes both MPI and hard-process contaminations: the trans-diff is hence the clearest measure of those contaminations. The comparisons to MC models are again made in these plots.

There is significant variation in performance between the models, with PYTHIA 8’s Monash tune and HERWIG 7 giving the best description of data in the plateau region of trans-min, followed within 10% by the other PYTHIA 8 tunes. EPOS, however, slightly overestimates in the “ramp” region to the pedestal effect plateau, and on the plateau it underestimates the pedestal height by around 20%. HERWIG 7 and PYTHIA 8 A2 both mismodel the transition, with a severe undershoot for HERWIG below p_T^{lead} of 5 GeV, and a milder but broader undershoot from A2 which extends up to $p_T^{\text{lead}} \approx 20 \text{ GeV}$.

The predictions cluster together more tightly in the process-inclusive trans-max region, with all generators other than EPOS providing a description of the N_{ch} density data within a few percent for $p_T^{\text{lead}} \geq 10 \text{ GeV}$; EPOS continues to undershoot the data significantly. PYTHIA 8 A14 also significantly undershoots the $\sum p_T$ density data, by around 10% as compared to EPOS’s 20%. Looking in trans-diff gives a clearer view of how non-MPI contributions to the UE are modelled, with mostly flat $\sim 10\%$ overshoots from all models other than EPOS in N_{ch} density, and a spread of performance in describing the $\sum p_T$ density evolution. In the latter the best performance comes from the PYTHIA 8 Monash and A2 tunes, with HERWIG 7 and PYTHIA 8 A14 both wrong by 5–10% but in opposite directions – EPOS’s prediction is again separated from the ATLAS data by more than 20%.

There is no obvious best model for all observables, but the PYTHIA 8 Monash tune agrees well with the data in all observables other than trans-diff N_{ch} density, and HERWIG 7 has comparable performance for hard-scattering events away from the “minimum-bias region” of $p_T^{\text{lead}} < 5 \text{ GeV}$. The PYTHIA 8 A14 tune, used for much of the hard-process simulation in ATLAS, predicts activity 5% to 10% below the data, indicating that some re-tuning for 13 TeV event modelling may yield performance benefits. EPOS is not able to model the level of underlying-event activity well in events with higher p_T^{lead} .

Mean transverse momentum in transverse & trans/min/max regions The per-event mean transverse momentum of charged particles in the transverse azimuthal regions is of interest since it illustrates the balance in UE physics between the $\sum p_T$ and multiplicity observables. This balance is affected in some MC models by colour-reconnection or -disruption mechanisms, which stochastically reconfigure the colour structures in the hadronising system into energetically favourable states and typically increase the p_T per particle. Measurements of the correlations of mean p_T with other event features are an important input to constrain such *ad hoc* models. Figure 6 shows, for the transverse and trans-min/max azimuthal regions,

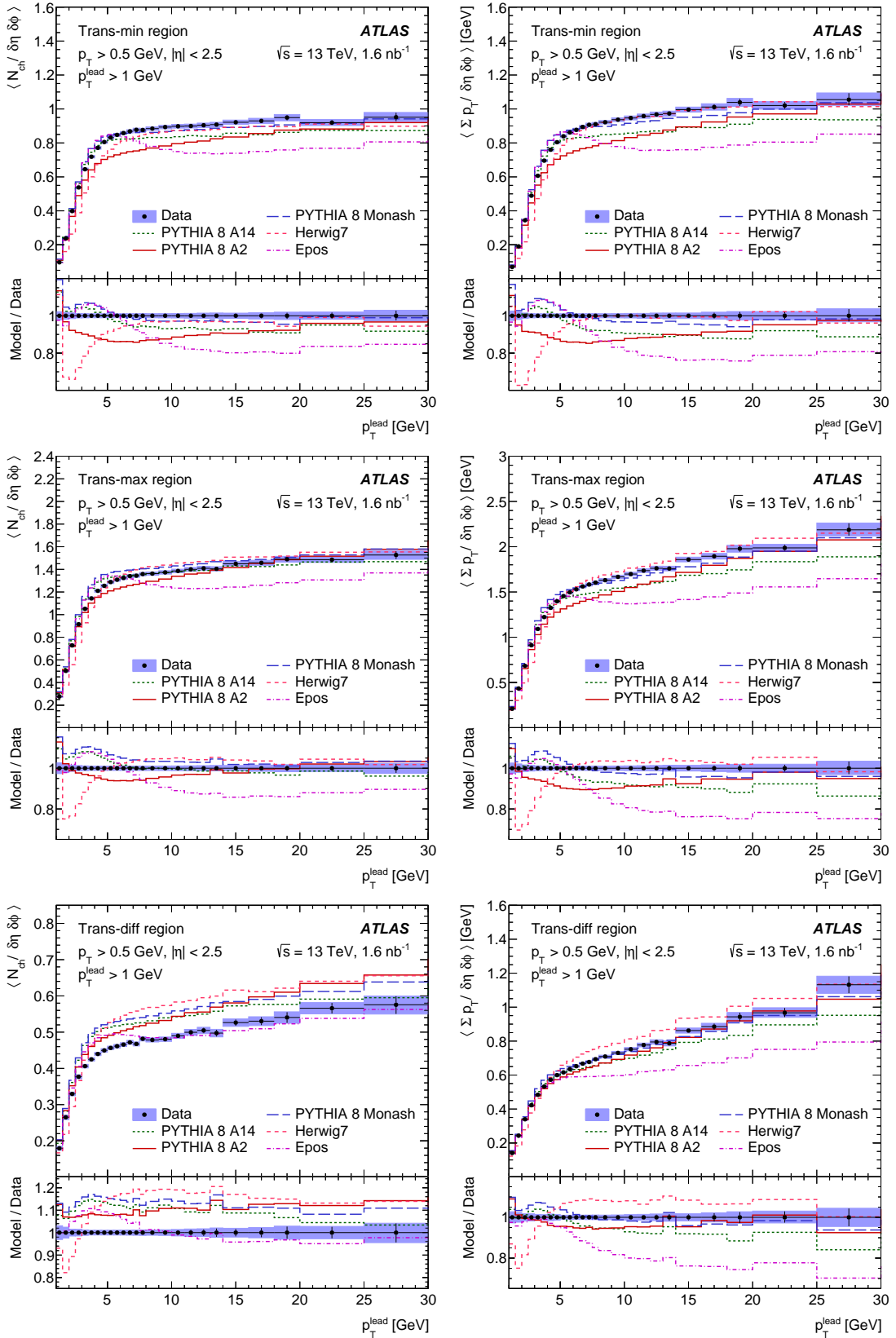


Figure 5: Mean densities of charged-particle multiplicity N_{ch} (left) and $\sum p_T$ (right) as a function of leading charged-particle p_T , in the trans-min (top), trans-max (middle) and trans-diff (bottom) azimuthal regions. The error bars on data points represent statistical uncertainty and the blue band the total combined statistical and systematic uncertainty.

the correlations of the average per-event mean transverse momentum, $\langle \text{mean } p_T \rangle$, with the transverse region's charged-particle multiplicity and the event's p_T^{lead} .

The correlation with transverse charged-particle multiplicity N_{ch} is a correlation between two different “soft” properties. This distribution is modelled to within 5% for all N_{ch} by most of the generators and in all transverse region variants, but in all cases an underestimation of $\langle \text{mean } p_T \rangle$ is visible until $N_{\text{ch}} \gtrsim 15$. The best modelling is from Epos, whose maximum undershoot is $\sim 3\%$ at low N_{ch} but which follows the data closely in all region definitions for higher transverse multiplicities. The Monash tune is the best-performing PYTHIA 8 configuration, with a performance similar to that of Epos, while PYTHIA 8 A14 undershoots in the low-multiplicity events and PYTHIA 8 A2 overshoots at high-multiplicities – notably the regions not included in each tune’s construction. HERWIG 7 shows the largest variations, from a $\sim 7\%$ undershoot at low N_{ch} to a 5% overshoot at $N_{\text{ch}} \approx 30$.

However, HERWIG 7 performs better than all the other generators when considering the correlation between transverse region $\langle \text{mean } p_T \rangle$ and p_T^{lead} . As seen in Figure 5, the transverse $\sum p_T$ does not reach as flat a plateau as does N_{ch} with increasing p_T^{lead} , and hence the event-wise $\langle \text{mean } p_T \rangle$ increases with p_T^{lead} . HERWIG’s behaviour in this observable is within 1% of the data except in the “minimum bias” $p_T^{\text{lead}} \lesssim 5 \text{ GeV}$ phase space (where the HERWIG model is not expected to work), while all PYTHIA 8 tunes undershoot the data by between 5% and 10%, and Epos even more so.

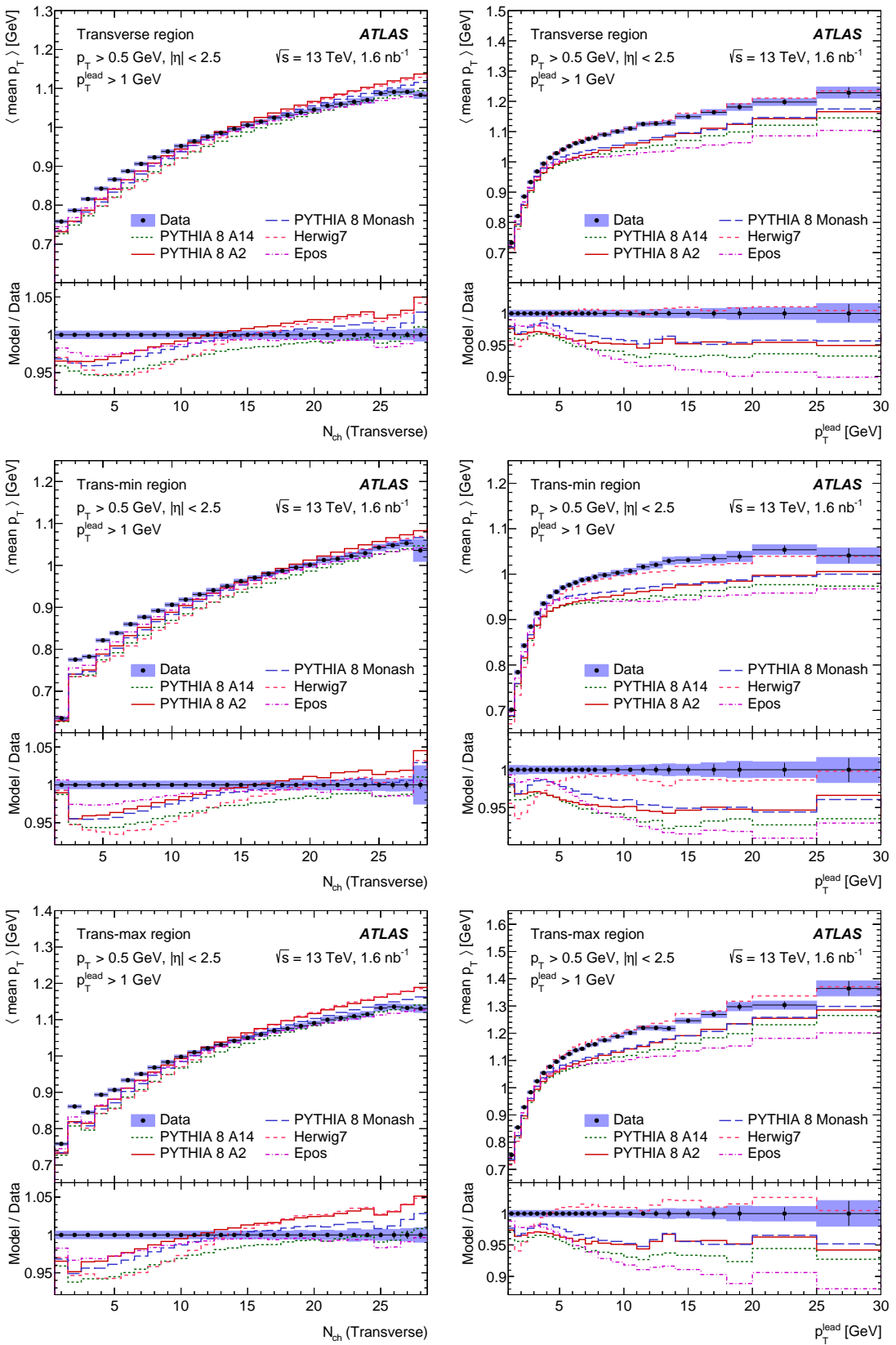


Figure 6: Mean charged-particle average transverse momentum as a function of charged-particle multiplicity in transverse region $N_{\text{ch}}(\text{Transverse})$ (left) and as a function of p_T^{lead} (right), for each of the transverse (top), trans-min (middle) and trans-max (bottom) azimuthal regions. The error bars on data points represent statistical uncertainty and the blue band the total combined statistical and systematic uncertainty.

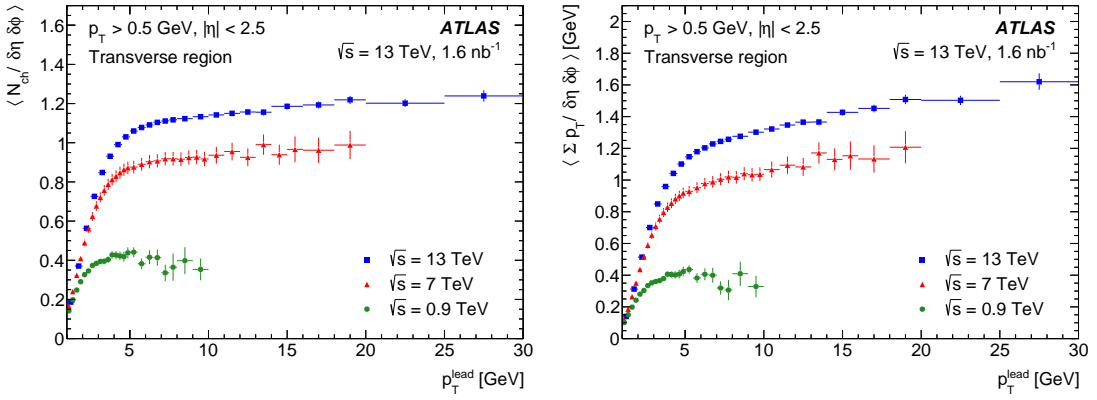


Figure 7: Mean charged-particle multiplicity (left) and $\sum p_T$ (right) densities as a function of transverse momentum of the leading charged particle measured for $\sqrt{s} = 0.9, 7$ TeV [1] and 13 TeV centre-of-mass energies. The fiducial acceptance definitions of the $\sqrt{s} = 0.9$ and 7 TeV measurements did not exclude charged strange baryons, but this effect is limited to a few percent at most.

9 Conclusions

We have presented several distributions sensitive to properties of the underlying event, measured by the ATLAS experiment at the LHC using 1.6 nb^{-1} of low-luminosity 13 TeV pp collision events. The measured observables are defined using charged tracks and have been corrected to the level of primary charged particles. Correction of the results for detector effects was performed via a combination of tracking and vertexing efficiency weighting and HBOM unfolding, with the latter accounting for re-orientation and similar indirect effects not accounted for by the reweighting. Systematic uncertainties are included for the effects of all data processing steps, including the unfolding.

The analysis observables follow the established strategy in which each event is azimuthally segmented into “towards”, “transverse”, and “away” regions with respect to the highest- p_T (“leading”) charged particle, with a further per-event distinction into “min” and “max” sides within the transverse region. This construction produces a set of observables collectively sensitive to each of the components of the underlying event. The observables in this study characterise the correlations of a) each azimuthal region’s mean $\sum p_T$ and mean charged-particle multiplicity densities with the transverse momentum, p_T^{lead} , of the event’s leading charged particle; and b) the per-event mean charged-particle p_T with both p_T^{lead} and the transverse azimuthal region’s charged-particle multiplicity. The correlations with p_T^{lead} characterise the degree of connection between the underlying event and the hardest partonic scattering in the pp collision, while correlations with the transverse regions’ charged-particle multiplicities probe the particle production mechanisms between underlying-event components.

The presented measurement improves upon previous ATLAS measurements of the underlying event using leading-track alignment, both in the reach in p_T^{lead} and the precision achieved. Figure 7 shows the transverse region’s mean N_{ch} and $\sum p_T$ densities in bins of p_T^{lead} as measured in leading-charged-particle UE studies at $\sqrt{s} = 0.9$ and 7 TeV, compared with the new 13 TeV data. An increase in UE activity of approximately 20% is observed when going from 7 TeV to 13 TeV pp collisions.

These results are a crucial input to physics studies in LHC pp collisions throughout the 13 TeV run, since the underlying event is present in all inelastic collision processes. Comparisons against predictions

from several commonly used MC generator configurations indicate that for most observables the models describe the underlying-event data to better than 5% accuracy. But this level of variation is far greater than the experimental uncertainty of the measurements, and there is evidence of systematic mismodelling. The model defects are particularly acute in the transition from generic soft inelastic interactions – so-called “minimum bias” scattering – to secondary interactions in the presence of hard partonic scattering. Some improvement to MC tunes in light of these data will hence be of benefit to physics studies in LHC Run 2. The EPOS MC generator, specialised for simulation of inclusive soft QCD processes, displays particularly discrepant features as the p_T^{lead} scale increases, casting doubt on its suitability for modelling LHC multiple pp interactions despite currently providing the best description of minimum-bias data.

This study hence provides important data from the new collider energy frontier for the tuning of MC generators in LHC Run 2, and further incentives for the development of a nucleon collision model capable of describing collider data in both hard and soft scatterings and at multiple centre-of-mass energies.

Acknowledgements

We thank CERN for the very successful operation of the LHC, as well as the support staff from our institutions without whom ATLAS could not be operated efficiently.

We acknowledge the support of ANPCyT, Argentina; YerPhI, Armenia; ARC, Australia; BMWFW and FWF, Austria; ANAS, Azerbaijan; SSTC, Belarus; CNPq and FAPESP, Brazil; NSERC, NRC and CFI, Canada; CERN; CONICYT, Chile; CAS, MOST and NSFC, China; COLCIENCIAS, Colombia; MSMT CR, MPO CR and VSC CR, Czech Republic; DNRF and DNSRC, Denmark; IN2P3-CNRS, CEA-DSM/IRFU, France; GNSF, Georgia; BMBF, HGF, and MPG, Germany; GSRT, Greece; RGC, Hong Kong SAR, China; ISF, I-CORE and Benoziyo Center, Israel; INFN, Italy; MEXT and JSPS, Japan; CNRST, Morocco; FOM and NWO, Netherlands; RCN, Norway; MNiSW and NCN, Poland; FCT, Portugal; MNE/IFA, Romania; MES of Russia and NRC KI, Russian Federation; JINR; MESTD, Serbia; MSSR, Slovakia; ARRS and MIZŠ, Slovenia; DST/NRF, South Africa; MINECO, Spain; SRC and Wallenberg Foundation, Sweden; SERI, SNSF and Cantons of Bern and Geneva, Switzerland; MOST, Taiwan; TAEK, Turkey; STFC, United Kingdom; DOE and NSF, United States of America. In addition, individual groups and members have received support from BCKDF, the Canada Council, CANARIE, CRC, Compute Canada, FQRNT, and the Ontario Innovation Trust, Canada; EPLANET, ERC, ERDF, FP7, Horizon 2020 and Marie Skłodowska-Curie Actions, European Union; Investissements d’Avenir Labex and Idex, ANR, Région Auvergne and Fondation Partager le Savoir, France; DFG and AvH Foundation, Germany; Herakleitos, Thales and Aristeia programmes co-financed by EU-ESF and the Greek NSRF; BSF, GIF and Minerva, Israel; BRF, Norway; CERCA Programme Generalitat de Catalunya, Generalitat Valenciana, Spain; the Royal Society and Leverhulme Trust, United Kingdom.

The crucial computing support from all WLCG partners is acknowledged gratefully, in particular from CERN, the ATLAS Tier-1 facilities at TRIUMF (Canada), NDGF (Denmark, Norway, Sweden), CC-IN2P3 (France), KIT/GridKA (Germany), INFN-CNAF (Italy), NL-T1 (Netherlands), PIC (Spain), ASGC (Taiwan), RAL (UK) and BNL (USA), the Tier-2 facilities worldwide and large non-WLCG resource providers. Major contributors of computing resources are listed in Ref. [44].

References

- [1] ATLAS Collaboration, *Measurement of underlying event characteristics using charged particles in pp collisions at $\sqrt{s} = 900 \text{ GeV}$ and 7 TeV with the ATLAS detector*, *Phys. Rev. D* **83** (2011) 112001, arXiv: [1012.0791 \[hep-ex\]](#).
- [2] ATLAS Collaboration, *Measurements of underlying-event properties using neutral and charged particles in pp collisions at 900 GeV and 7 TeV with the ATLAS detector at the LHC*, *Eur. Phys. J. C* **71** (2011) 1636, arXiv: [1103.1816 \[hep-ex\]](#).
- [3] ATLAS Collaboration, *Underlying event characteristics and their dependence on jet size of charged-particle jet events in pp collisions at $\sqrt{s} = 7 \text{ TeV}$ with the ATLAS detector*, *Phys. Rev. D* **86** (2012) 072004, arXiv: [1208.0563 \[hep-ex\]](#).
- [4] ATLAS Collaboration, *Measurement of the underlying event in jet events from 7 TeV proton–proton collisions with the ATLAS detector*, *Eur. Phys. J. C* **74** (2014) 2965, arXiv: [1406.0392 \[hep-ex\]](#).
- [5] ATLAS Collaboration, *Measurement of distributions sensitive to the underlying event in inclusive Z-boson production in pp collisions at $\sqrt{s} = 7 \text{ TeV}$ with the ATLAS detector*, *Eur. Phys. J. C* **74** (2014) 3195, arXiv: [1409.3433 \[hep-ex\]](#).
- [6] ALICE Collaboration, B. Abelev et al., *Underlying event measurements in pp collisions at $\sqrt{s} = 0.9$ and 7 TeV with the ALICE experiment at the LHC*, *JHEP* **07** (2012) 116, arXiv: [1112.2082 \[hep-ex\]](#).
- [7] CMS Collaboration, *First measurement of the underlying event activity at the LHC with $\sqrt{s} = 0.9 \text{ TeV}$* , *Eur. Phys. J. C* **70** (2010) 555, arXiv: [1006.2083 \[hep-ex\]](#).
- [8] CMS Collaboration, *Measurement of the underlying event activity using charged-particle jets in proton–proton collisions at $\sqrt{s} = 2.76 \text{ TeV}$* , *JHEP* **09** (2015) 137, arXiv: [1507.07229 \[hep-ex\]](#).
- [9] CMS Collaboration, *Measurement of the underlying event in the Drell-Yan process in proton–proton collisions at $\sqrt{s} = 7 \text{ TeV}$* , *Eur. Phys. J. C* **72** (2012) 2080, arXiv: [1204.1411 \[hep-ex\]](#).
- [10] CDF Collaboration, T. Affolder et al., *Charged jet evolution and the underlying event in $p\bar{p}$ collisions at 1.8 TeV* , *Phys. Rev. D* **65** (2002) 092002.
- [11] CDF Collaboration, T. Affolder et al., *The underlying event in hard interactions at the Tevatron $\bar{p}p$ collider*, *Phys. Rev. D* **70** (2004) 072002, arXiv: [hep-ex/0404004 \[hep-ex\]](#).
- [12] CDF Collaboration, T. Aaltonen et al., *Studying the underlying event in Drell-Yan and high transverse momentum jet Production at the Tevatron*, *Phys. Rev. D* **82** (2010) 034001, arXiv: [1003.3146 \[hep-ex\]](#).
- [13] ATLAS Collaboration, *The ATLAS Experiment at the CERN Large Hadron Collider*, *JINST* **3** (2008) S08003.
- [14] ATLAS Collaboration, *Charged-particle distributions in $\sqrt{s} = 13 \text{ TeV}$ pp interactions measured with the ATLAS detector at the LHC*, *Phys. Lett. B* **758** (2016) 67, arXiv: [1602.01633 \[hep-ex\]](#).

- [15] G. Marchesini and B. R. Webber, *Associated transverse energy in hadronic jet production*, *Phys. Rev. D* **38** (1988) 3419.
- [16] J. Pumplin, *Hard underlying event correction to inclusive jet cross-sections*, *Phys. Rev. D* **57** (1998) 5787, arXiv: [hep-ph/9708464 \[hep-ph\]](#).
- [17] T. Sjöstrand, S. Mrenna and P. Z. Skands, *A brief introduction to PYTHIA 8.1*, *Comput. Phys. Commun.* **178** (2008) 852, arXiv: [0710.3820 \[hep-ph\]](#).
- [18] T. Sjöstrand, S. Mrenna and P. Z. Skands, *PYTHIA 6.4 Physics and Manual*, *JHEP* **05** (2006) 026, arXiv: [hep-ph/0603175 \[hep-ph\]](#).
- [19] J. Bellm et al., *Herwig 7.0/Herwig++ 3.0 release note*, *Eur. Phys. J. C* **76** (2016) 196, arXiv: [1512.01178 \[hep-ph\]](#).
- [20] T. Pierog and K. Werner, *EPOS model and ultra high energy cosmic rays*, *Nucl. Phys. Proc. Suppl.* **196** (2009) 102, arXiv: [0905.1198 \[hep-ph\]](#).
- [21] T. Pierog, I. Karpenko, J. M. Katzy, E. Yatsenko and K. Werner, *EPOS LHC: test of collective hadronization with data measured at the CERN Large Hadron Collider*, *Phys. Rev. C* **92** (2015) 034906, arXiv: [1306.0121 \[hep-ph\]](#).
- [22] T. Sjöstrand and M. van Zijl, *A Multiple Interaction Model for the Event Structure in Hadron Collisions*, *Phys. Rev. D* **36** (1987) 2019.
- [23] ATLAS Collaboration, *ATLAS PYTHIA 8 tunes to 7 TeV data*, ATL-PHYS-PUB-2014-021, 2014, URL: <https://cdsweb.cern.ch/record/1966419>.
- [24] NNPDF Collaboration, R. D. Ball et al., *Parton distributions with LHC data*, *Nucl. Phys. B* **867** (2013) 244, arXiv: [1207.1303 \[hep-ph\]](#).
- [25] P. Skands, S. Carrazza and J. Rojo, *Tuning PYTHIA 8.1: the Monash 2013 Tune*, *Eur. Phys. J. C* **74** (2014) 3024, arXiv: [1404.5630 \[hep-ph\]](#).
- [26] ATLAS Collaboration, *Charged-particle multiplicities in pp interactions measured with the ATLAS detector at the LHC*, *New J. Phys.* **13** (2011) 053033, arXiv: [1012.5104 \[hep-ex\]](#).
- [27] ATLAS Collaboration, *Charged-particle distributions in pp interactions at $\sqrt{s} = 8$ TeV measured with the ATLAS detector*, *Eur. Phys. J. C* **76** (2016) 403, arXiv: [1603.02439 \[hep-ex\]](#).
- [28] ATLAS Collaboration, *Further ATLAS tunes of PYTHIA 6 and PYTHIA 8*, ATL-PHYS-PUB-2011-014, 2011, URL: <https://cds.cern.ch/record/1400677>.
- [29] A. D. Martin, W. J. Stirling, R. S. Thorne and G. Watt, *Parton distributions for the LHC*, *Eur. Phys. J. C* **63** (2009) 189, arXiv: [0901.0002 \[hep-ph\]](#).
- [30] ATLAS Collaboration, *Measurements of the pseudorapidity dependence of the total transverse energy in proton–proton collisions at $\sqrt{s} = 7$ TeV with ATLAS*, *JHEP* **11** (2012) 033, arXiv: [1208.6256 \[hep-ex\]](#).
- [31] M. Bahr et al., *Herwig++ physics and manual*, *Eur. Phys. J. C* **58** (2008) 639, arXiv: [0803.0883 \[hep-ph\]](#).
- [32] M. Bahr, J. M. Butterworth and M. H. Seymour, *The Underlying Event and the Total Cross Section from Tevatron to the LHC*, *JHEP* **01** (2009) 065, arXiv: [0806.2949 \[hep-ph\]](#).

- [33] L. A. Harland-Lang, A. D. Martin, P. Motylinski and R. S. Thorne, *Parton distributions in the LHC era: MMHT 2014 PDFs*, *Eur. Phys. J. C* **75** (2015) 204, arXiv: [1412.3989 \[hep-ph\]](https://arxiv.org/abs/1412.3989).
- [34] M. H. Seymour and A. Siodmok, *Constraining MPI models using σ_{eff} and recent Tevatron and LHC underlying event data*, *JHEP* **10** (2013) 113, arXiv: [1307.5015 \[hep-ph\]](https://arxiv.org/abs/1307.5015).
- [35] ATLAS Collaboration, *The ATLAS simulation infrastructure*, *Eur. Phys. J. C* **70** (2010) 823, arXiv: [1005.4568 \[physics.ins-det\]](https://arxiv.org/abs/1005.4568).
- [36] S. Agostinelli et al., *GEANT 4: a simulation toolkit*, *Nucl. Instrum. Meth. A* **506** (2003) 250.
- [37] M Capeans et al., *ATLAS Insertable B-Layer Technical Design Report*, CERN-LHCC-2010-013, 2010, URL: <https://cds.cern.ch/record/1291633>.
- [38] ATLAS Collaboration, *2015 start-up trigger menu and initial performance assessment of the ATLAS trigger using Run-2 data*, ATL-DAQ-PUB-2016-001, 2016, URL: <https://cds.cern.ch/record/2136007>.
- [39] G. Piacquadio, K. Prokofiev and A. Wildauer, *Primary vertex reconstruction in the ATLAS experiment at LHC*, *J. Phys. Conf. Ser.* **119** (2008) 032033.
- [40] ALICE Collaboration, K. Aamodt et al., *Strange particle production in proton–proton collisions at $\sqrt{s} = 0.9 \text{ TeV}$ with ALICE at the LHC*, *Eur. Phys. J. C* **71** (2011) 1594, arXiv: [1012.3257 \[hep-ex\]](https://arxiv.org/abs/1012.3257).
- [41] J. W. Monk and C. Oropeza-Barrera, *The HBOM method for unfolding detector effects*, *Nucl. Instrum. Meth. A* **701** (2013) 17, arXiv: [1111.4896 \[hep-ex\]](https://arxiv.org/abs/1111.4896).
- [42] G. D’Agostini, *A multidimensional unfolding method based on Bayes’ theorem*, *Nucl. Instr. Meth. A* **362** (1995) 487.
- [43] A. Buckley et al., *Rivet user manual*, *Comput. Phys. Commun.* **184** (2013) 2803, arXiv: [1003.0694 \[hep-ph\]](https://arxiv.org/abs/1003.0694).
- [44] ATLAS Collaboration, *ATLAS Computing Acknowledgements 2016–2017*, ATL-GEN-PUB-2016-002, 2016, URL: <https://cds.cern.ch/record/2202407>.

The ATLAS Collaboration

M. Aaboud^{137d}, G. Aad⁸⁸, B. Abbott¹¹⁵, J. Abdallah⁸, O. Abdinov¹², B. Abelos¹¹⁹, S.H. Abidi¹⁶¹, O.S. AbouZeid¹³⁹, N.L. Abraham¹⁵¹, H. Abramowicz¹⁵⁵, H. Abreu¹⁵⁴, R. Abreu¹¹⁸, Y. Abulaiti^{148a,148b}, B.S. Acharya^{167a,167b,a}, S. Adachi¹⁵⁷, L. Adamczyk^{41a}, D.L. Adams²⁷, J. Adelman¹¹⁰, M. Adersberger¹⁰², T. Adye¹³³, A.A. Affolder¹³⁹, T. Agatonovic-Jovin¹⁴, C. Agheorghiesei^{28b}, J.A. Aguilar-Saavedra^{128a,128f}, S.P. Ahlen²⁴, F. Ahmadov^{68,b}, G. Aielli^{135a,135b}, S. Akatsuka⁷¹, H. Akerstedt^{148a,148b}, T.P.A. Åkesson⁸⁴, A.V. Akimov⁹⁸, G.L. Alberghi^{22a,22b}, J. Albert¹⁷², M.J. Alconada Verzini⁷⁴, M. Aleksa³², I.N. Aleksandrov⁶⁸, C. Alexa^{28b}, G. Alexander¹⁵⁵, T. Alexopoulos¹⁰, M. Alhroob¹¹⁵, B. Ali¹³⁰, M. Aliev^{76a,76b}, G. Alimonti^{94a}, J. Alison³³, S.P. Alkire³⁸, B.M.M. Allbrooke¹⁵¹, B.W. Allen¹¹⁸, P.P. Allport¹⁹, A. Aloisio^{106a,106b}, A. Alonso³⁹, F. Alonso⁷⁴, C. Alpigiani¹⁴⁰, A.A. Alshehri⁵⁶, M. Alstaty⁸⁸, B. Alvarez Gonzalez³², D. Álvarez Piqueras¹⁷⁰, M.G. Alvaggi^{106a,106b}, B.T. Amadio¹⁶, Y. Amaral Coutinho^{26a}, C. Amelung²⁵, D. Amidei⁹², S.P. Amor Dos Santos^{128a,128c}, A. Amorim^{128a,128b}, S. Amoroso³², G. Amundsen²⁵, C. Anastopoulos¹⁴¹, L.S. Ancu⁵², N. Andari¹⁹, T. Andeen¹¹, C.F. Anders^{60b}, J.K. Anders⁷⁷, K.J. Anderson³³, A. Andreazza^{94a,94b}, V. Andrei^{60a}, S. Angelidakis⁹, I. Angelozzi¹⁰⁹, A. Angerami³⁸, F. Anghinolfi³², A.V. Anisenkov^{111,c}, N. Anjos¹³, A. Annovi^{126a,126b}, C. Antel^{60a}, M. Antonelli⁵⁰, A. Antonov^{100,*}, D.J. Antrim¹⁶⁶, F. Anulli^{134a}, M. Aoki⁶⁹, L. Aperio Bella³², G. Arabidze⁹³, Y. Arai⁶⁹, J.P. Araque^{128a}, V. Araujo Ferraz^{26a}, A.T.H. Arce⁴⁸, R.E. Ardell⁸⁰, F.A. Arduh⁷⁴, J.-F. Arguin⁹⁷, S. Argyropoulos⁶⁶, M. Arik^{20a}, A.J. Armbruster¹⁴⁵, L.J. Armitage⁷⁹, O. Arnaez³², H. Arnold⁵¹, M. Arratia³⁰, O. Arslan²³, A. Artamonov⁹⁹, G. Artoni¹²², S. Artz⁸⁶, S. Asai¹⁵⁷, N. Asbah⁴⁵, A. Ashkenazi¹⁵⁵, L. Asquith¹⁵¹, K. Assamagan²⁷, R. Astalos^{146a}, M. Atkinson¹⁶⁹, N.B. Atlay¹⁴³, K. Augsten¹³⁰, G. Avolio³², B. Axen¹⁶, M.K. Ayoub¹¹⁹, G. Azuelos^{97,d}, A.E. Baas^{60a}, M.J. Baca¹⁹, H. Bachacou¹³⁸, K. Bachas^{76a,76b}, M. Backes¹²², M. Backhaus³², P. Bagiacchi^{134a,134b}, P. Bagnaia^{134a,134b}, J.T. Baines¹³³, M. Bajic³⁹, O.K. Baker¹⁷⁹, E.M. Baldin^{111,c}, P. Balek¹⁷⁵, T. Balestri¹⁵⁰, F. Balli¹³⁸, W.K. Balunas¹²⁴, E. Banas⁴², Sw. Banerjee^{176,e}, A.A.E. Bannoura¹⁷⁸, L. Barak³², E.L. Barberio⁹¹, D. Barberis^{53a,53b}, M. Barbero⁸⁸, T. Barillari¹⁰³, M-S Barisits³², T. Barklow¹⁴⁵, N. Barlow³⁰, S.L. Barnes^{36c}, B.M. Barnett¹³³, R.M. Barnett¹⁶, Z. Barnovska-Blenessy^{36a}, A. Baroncelli^{136a}, G. Barone²⁵, A.J. Barr¹²², L. Barranco Navarro¹⁷⁰, F. Barreiro⁸⁵, J. Barreiro Guimarães da Costa^{35a}, R. Bartoldus¹⁴⁵, A.E. Barton⁷⁵, P. Bartos^{146a}, A. Basalaev¹²⁵, A. Bassalat^{119,f}, R.L. Bates⁵⁶, S.J. Batista¹⁶¹, J.R. Batley³⁰, M. Battaglia¹³⁹, M. Bauce^{134a,134b}, F. Bauer¹³⁸, H.S. Bawa^{145,g}, J.B. Beacham¹¹³, M.D. Beattie⁷⁵, T. Beau⁸³, P.H. Beauchemin¹⁶⁵, P. Bechtle²³, H.P. Beck^{18,h}, K. Becker¹²², M. Becker⁸⁶, M. Beckingham¹⁷³, C. Becot¹¹², A.J. Beddall^{20e}, A. Beddall^{20b}, V.A. Bednyakov⁶⁸, M. Bedognetti¹⁰⁹, C.P. Bee¹⁵⁰, T.A. Beermann³², M. Begalli^{26a}, M. Begel²⁷, J.K. Behr⁴⁵, A.S. Bell⁸¹, G. Bella¹⁵⁵, L. Bellagamba^{22a}, A. Bellerive³¹, M. Bellomo⁸⁹, K. Belotskiy¹⁰⁰, O. Beltramello³², N.L. Belyaev¹⁰⁰, O. Benary^{155,*}, D. Bencheikoun^{137a}, M. Bender¹⁰², K. Bendtz^{148a,148b}, N. Benekos¹⁰, Y. Benhammou¹⁵⁵, E. Benhar Noccioli¹⁷⁹, J. Benitez⁶⁶, D.P. Benjamin⁴⁸, M. Benoit⁵², J.R. Bensinger²⁵, S. Bentvelsen¹⁰⁹, L. Beresford¹²², M. Beretta⁵⁰, D. Berge¹⁰⁹, E. Bergeaas Kuutmann¹⁶⁸, N. Berger⁵, J. Beringer¹⁶, S. Berlendis⁵⁸, N.R. Bernard⁸⁹, G. Bernardi⁸³, C. Bernius¹¹², F.U. Bernlochner²³, T. Berry⁸⁰, P. Berta¹³¹, C. Bertella⁸⁶, G. Bertoli^{148a,148b}, F. Bertolucci^{126a,126b}, I.A. Bertram⁷⁵, C. Bertsche⁴⁵, D. Bertsche¹¹⁵, G.J. Besjes³⁹, O. Bessidskaia Bylund^{148a,148b}, M. Bessner⁴⁵, N. Besson¹³⁸, C. Betancourt⁵¹, A. Bethani⁸⁷, S. Bethke¹⁰³, A.J. Bevan⁷⁹, R.M. Bianchi¹²⁷, M. Bianco³², O. Biebel¹⁰², D. Biedermann¹⁷, R. Bielski⁸⁷, N.V. Biesuz^{126a,126b}, M. Biglietti^{136a}, J. Bilbao De Mendizabal⁵², T.R.V. Billoud⁹⁷, H. Bilokon⁵⁰, M. Bindi⁵⁷, A. Bingul^{20b}, C. Bini^{134a,134b}, S. Biondi^{22a,22b}, T. Bisanz⁵⁷, C. Bitrich⁴⁷, D.M. Bjergaard⁴⁸, C.W. Black¹⁵², J.E. Black¹⁴⁵, K.M. Black²⁴, D. Blackburn¹⁴⁰, R.E. Blair⁶, T. Blazek^{146a}, I. Bloch⁴⁵, C. Blocker²⁵, A. Blue⁵⁶, W. Blum^{86,*}, U. Blumenschein⁷⁹, S. Blunier^{34a},

G.J. Bobbink¹⁰⁹, V.S. Bobrovnikov^{111,c}, S.S. Bocchetta⁸⁴, A. Bocci⁴⁸, C. Bock¹⁰², M. Boehler⁵¹, D. Boerner¹⁷⁸, D. Bogavac¹⁰², A.G. Bogdanchikov¹¹¹, C. Bohm^{148a}, V. Boisvert⁸⁰, P. Bokan¹⁶⁸, T. Bold^{41a}, A.S. Boldyrev¹⁰¹, M. Bomben⁸³, M. Bona⁷⁹, M. Boonekamp¹³⁸, A. Borisov¹³², G. Borissov⁷⁵, J. Bortfeldt³², D. Bortolotto¹²², V. Bortolotto^{62a,62b,62c}, K. Bos¹⁰⁹, D. Boscherini^{22a}, M. Bosman¹³, J.D. Bossio Sola²⁹, J. Boudreau¹²⁷, J. Bouffard², E.V. Bouhova-Thacker⁷⁵, D. Boumediene³⁷, C. Bourdarios¹¹⁹, S.K. Boutle⁵⁶, A. Boveia¹¹³, J. Boyd³², I.R. Boyko⁶⁸, J. Bracinik¹⁹, A. Brandt⁸, G. Brandt⁵⁷, O. Brandt^{60a}, U. Bratzler¹⁵⁸, B. Brau⁸⁹, J.E. Brau¹¹⁸, W.D. Breaden Madden⁵⁶, K. Brendlinger⁴⁵, A.J. Brennan⁹¹, L. Brenner¹⁰⁹, R. Brenner¹⁶⁸, S. Bressler¹⁷⁵, D.L. Briglin¹⁹, T.M. Bristow⁴⁹, D. Britton⁵⁶, D. Britzger⁴⁵, F.M. Brochu³⁰, I. Brock²³, R. Brock⁹³, G. Brooijmans³⁸, T. Brooks⁸⁰, W.K. Brooks^{34b}, J. Brosamer¹⁶, E. Brost¹¹⁰, J.H. Broughton¹⁹, P.A. Bruckman de Renstrom⁴², D. Bruncko^{146b}, A. Bruni^{22a}, G. Bruni^{22a}, L.S. Bruni¹⁰⁹, BH Brunt³⁰, M. Bruschi^{22a}, N. Bruscino²³, P. Bryant³³, L. Bryngemark⁸⁴, T. Buanes¹⁵, Q. Buat¹⁴⁴, P. Buchholz¹⁴³, A.G. Buckley⁵⁶, I.A. Budagov⁶⁸, F. Buehrer⁵¹, M.K. Bugge¹²¹, O. Bulekov¹⁰⁰, D. Bullock⁸, H. Burckhart³², S. Burdin⁷⁷, C.D. Burgard⁵¹, A.M. Burger⁵, B. Burghgrave¹¹⁰, K. Burka⁴², S. Burke¹³³, I. Burmeister⁴⁶, J.T.P. Burr¹²², E. Busato³⁷, D. Büscher⁵¹, V. Büscher⁸⁶, P. Bussey⁵⁶, J.M. Butler²⁴, C.M. Buttar⁵⁶, J.M. Butterworth⁸¹, P. Butti¹⁰⁹, W. Buttinger²⁷, A. Buzatu^{35c}, A.R. Buzykaev^{111,c}, S. Cabrera Urbán¹⁷⁰, D. Caforio¹³⁰, V.M. Cairo^{40a,40b}, O. Cakir^{4a}, N. Calace⁵², P. Calafuria¹⁶, A. Calandri⁸⁸, G. Calderini⁸³, P. Calfayan⁶⁴, G. Callea^{40a,40b}, L.P. Caloba^{26a}, S. Calvente Lopez⁸⁵, D. Calvet³⁷, S. Calvet³⁷, T.P. Calvet⁸⁸, R. Camacho Toro³³, S. Camarda³², P. Camarri^{135a,135b}, D. Cameron¹²¹, R. Caminal Armadans¹⁶⁹, C. Camincher⁵⁸, S. Campana³², M. Campanelli⁸¹, A. Camplani^{94a,94b}, A. Campoverde¹⁴³, V. Canale^{106a,106b}, M. Cano Bret^{36c}, J. Cantero¹¹⁶, T. Cao¹⁵⁵, M.D.M. Capeans Garrido³², I. Caprini^{28b}, M. Caprini^{28b}, M. Capua^{40a,40b}, R.M. Carbone³⁸, R. Cardarelli^{135a}, F. Cardillo⁵¹, I. Carli¹³¹, T. Carli³², G. Carlino^{106a}, B.T. Carlson¹²⁷, L. Carminati^{94a,94b}, R.M.D. Carney^{148a,148b}, S. Caron¹⁰⁸, E. Carquin^{34b}, G.D. Carrillo-Montoya³², J. Carvalho^{128a,128c}, D. Casadei¹⁹, M.P. Casado^{13,i}, M. Casolino¹³, D.W. Casper¹⁶⁶, R. Castelijn¹⁰⁹, A. Castelli¹⁰⁹, V. Castillo Gimenez¹⁷⁰, N.F. Castro^{128a,j}, A. Catinaccio³², J.R. Catmore¹²¹, A. Cattai³², J. Caudron²³, V. Cavalieri¹⁶⁹, E. Cavallaro¹³, D. Cavalli^{94a}, M. Cavalli-Sforza¹³, V. Cavasinni^{126a,126b}, E. Celebi^{20a}, F. Ceradini^{136a,136b}, L. Cerdá Alberich¹⁷⁰, A.S. Cerqueira^{26b}, A. Cerri¹⁵¹, L. Cerrito^{135a,135b}, F. Cerutti¹⁶, A. Cervelli¹⁸, S.A. Cetin^{20d}, A. Chafaq^{137a}, D. Chakraborty¹¹⁰, S.K. Chan⁵⁹, W.S. Chan¹⁰⁹, Y.L. Chan^{62a}, P. Chang¹⁶⁹, J.D. Chapman³⁰, D.G. Charlton¹⁹, A. Chatterjee⁵², C.C. Chau¹⁶¹, C.A. Chavez Barajas¹⁵¹, S. Che¹¹³, S. Cheatham^{167a,167c}, A. Chegwidden⁹³, S. Chekanov⁶, S.V. Chekulaev^{163a}, G.A. Chelkov^{68,k}, M.A. Chelstowska³², C. Chen⁶⁷, H. Chen²⁷, S. Chen^{35b}, S. Chen¹⁵⁷, X. Chen^{35c,l}, Y. Chen⁷⁰, H.C. Cheng⁹², H.J. Cheng^{35a}, Y. Cheng³³, A. Cheplakov⁶⁸, E. Cheremushkina¹³², R. Cherkaoui El Moursli^{137e}, V. Chernyatin^{27,*}, E. Cheu⁷, L. Chevalier¹³⁸, V. Chiarella⁵⁰, G. Chiarelli^{126a,126b}, G. Chiodini^{76a}, A.S. Chisholm³², A. Chitan^{28b}, Y.H. Chiu¹⁷², M.V. Chizhov⁶⁸, K. Choi⁶⁴, A.R. Chomont³⁷, S. Chouridou⁹, B.K.B. Chow¹⁰², V. Christodoulou⁸¹, D. Chromek-Burckhart³², M.C. Chu^{62a}, J. Chudoba¹²⁹, A.J. Chuinard⁹⁰, J.J. Chwastowski⁴², L. Chytka¹¹⁷, A.K. Ciftci^{4a}, D. Cinca⁴⁶, V. Cindro⁷⁸, I.A. Cioara²³, C. Ciocca^{22a,22b}, A. Ciocio¹⁶, F. Cirotto^{106a,106b}, Z.H. Citron¹⁷⁵, M. Citterio^{94a}, M. Ciubancan^{28b}, A. Clark⁵², B.L. Clark⁵⁹, M.R. Clark³⁸, P.J. Clark⁴⁹, R.N. Clarke¹⁶, C. Clement^{148a,148b}, Y. Coadou⁸⁸, M. Cobal^{167a,167c}, A. Coccaro⁵², J. Cochran⁶⁷, L. Colasurdo¹⁰⁸, B. Cole³⁸, A.P. Colijn¹⁰⁹, J. Collot⁵⁸, T. Colombo¹⁶⁶, P. Conde Muiño^{128a,128b}, E. Coniavitis⁵¹, S.H. Connell^{147b}, I.A. Connolly⁸⁷, V. Consorti⁵¹, S. Constantinescu^{28b}, G. Conti³², F. Conventi^{106a,m}, M. Cooke¹⁶, B.D. Cooper⁸¹, A.M. Cooper-Sarkar¹²², F. Cormier¹⁷¹, K.J.R. Cormier¹⁶¹, T. Cornelissen¹⁷⁸, M. Corradi^{134a,134b}, F. Corriveau^{90,n}, A. Cortes-Gonzalez³², G. Cortiana¹⁰³, G. Costa^{94a}, M.J. Costa¹⁷⁰, D. Costanzo¹⁴¹, G. Cottin³⁰, G. Cowan⁸⁰, B.E. Cox⁸⁷, K. Cranmer¹¹², S.J. Crawley⁵⁶, R.A. Creager¹²⁴, G. Cree³¹, S. Crépé-Renaudin⁵⁸, F. Crescioli⁸³, W.A. Cribbs^{148a,148b}, M. Crispin Ortuzar¹²², M. Cristinziani²³,

V. Croft¹⁰⁸, G. Crosetti^{40a,40b}, A. Cueto⁸⁵, T. Cuhadar Donszelmann¹⁴¹, J. Cummings¹⁷⁹, M. Curatolo⁵⁰, J. Cúth⁸⁶, H. Czirr¹⁴³, P. Czodrowski³², G. D'amen^{22a,22b}, S. D'Auria⁵⁶, M. D'Onofrio⁷⁷, M.J. Da Cunha Sargedas De Sousa^{128a,128b}, C. Da Via⁸⁷, W. Dabrowski^{41a}, T. Dado^{146a}, T. Dai⁹², O. Dale¹⁵, F. Dallaire⁹⁷, C. Dallapiccola⁸⁹, M. Dam³⁹, J.R. Dandoy¹²⁴, N.P. Dang⁵¹, A.C. Daniells¹⁹, N.S. Dann⁸⁷, M. Danninger¹⁷¹, M. Dano Hoffmann¹³⁸, V. Dao¹⁵⁰, G. Darbo^{53a}, S. Darmora⁸, J. Dassoulas³, A. Dattagupta¹¹⁸, T. Daubney⁴⁵, W. Davey²³, C. David⁴⁵, T. Davidek¹³¹, M. Davies¹⁵⁵, P. Davison⁸¹, E. Dawe⁹¹, I. Dawson¹⁴¹, K. De⁸, R. de Asmundis^{106a}, A. De Benedetti¹¹⁵, S. De Castro^{22a,22b}, S. De Cecco⁸³, N. De Groot¹⁰⁸, P. de Jong¹⁰⁹, H. De la Torre⁹³, F. De Lorenzi⁶⁷, A. De Maria⁵⁷, D. De Pedis^{134a}, A. De Salvo^{134a}, U. De Sanctis¹⁵¹, A. De Santo¹⁵¹, K. De Vasconcelos Corga⁸⁸, J.B. De Vivie De Regie¹¹⁹, W.J. Dearnaley⁷⁵, R. Debbe²⁷, C. Debenedetti¹³⁹, D.V. Dedovich⁶⁸, N. Dehghanian³, I. Deigaard¹⁰⁹, M. Del Gaudio^{40a,40b}, J. Del Peso⁸⁵, T. Del Prete^{126a,126b}, D. Delgove¹¹⁹, F. Deliot¹³⁸, C.M. Delitzsch⁵², A. Dell' Acqua³², L. Dell'Asta²⁴, M. Dell' Orso^{126a,126b}, M. Della Pietra^{106a,m}, D. della Volpe⁵², M. Delmastro⁵, P.A. Delsart⁵⁸, D.A. DeMarco¹⁶¹, S. Demers¹⁷⁹, M. Demichev⁶⁸, A. Demilly⁸³, S.P. Denisov¹³², D. Denysiuk¹³⁸, D. Derendarz⁴², J.E. Derkaoui^{137d}, F. Derue⁸³, P. Dervan⁷⁷, K. Desch²³, C. Deterre⁴⁵, K. Dette⁴⁶, P.O. Deviveiros³², A. Dewhurst¹³³, S. Dhaliwal²⁵, A. Di Ciaccio^{135a,135b}, L. Di Ciaccio⁵, W.K. Di Clemente¹²⁴, C. Di Donato^{106a,106b}, A. Di Girolamo³², B. Di Girolamo³², B. Di Micco^{136a,136b}, R. Di Nardo³², K.F. Di Petrillo⁵⁹, A. Di Simone⁵¹, R. Di Sipio¹⁶¹, D. Di Valentino³¹, C. Diaconu⁸⁸, M. Diamond¹⁶¹, F.A. Dias⁴⁹, M.A. Diaz^{34a}, E.B. Diehl⁹², J. Dietrich¹⁷, S. Díez Cornell⁴⁵, A. Dimitrievska¹⁴, J. Dingfelder²³, P. Dita^{28b}, S. Dita^{28b}, F. Dittus³², F. Djama⁸⁸, T. Djobava^{54b}, J.I. Djuvtsland^{60a}, M.A.B. do Vale^{26c}, D. Dobos³², M. Dobre^{28b}, C. Doglioni⁸⁴, J. Dolejsi¹³¹, Z. Dolezal¹³¹, M. Donadelli^{26d}, S. Donati^{126a,126b}, P. Dondero^{123a,123b}, J. Donini³⁷, J. Dopke¹³³, A. Doria^{106a}, M.T. Dova⁷⁴, A.T. Doyle⁵⁶, E. Drechsler⁵⁷, M. Dris¹⁰, Y. Du^{36b}, J. Duarte-Campderros¹⁵⁵, E. Duchovni¹⁷⁵, G. Duckeck¹⁰², O.A. Ducu^{97,o}, D. Duda¹⁰⁹, A. Dudarev³², A.Chr. Dudder⁸⁶, E.M. Duffield¹⁶, L. Duflot¹¹⁹, M. Dührssen³², M. Dumancic¹⁷⁵, A.E. Dumitriu^{28b}, A.K. Duncan⁵⁶, M. Dunford^{60a}, H. Duran Yildiz^{4a}, M. Düren⁵⁵, A. Durglishvili^{54b}, D. Duschinger⁴⁷, B. Dutta⁴⁵, M. Dyndal⁴⁵, C. Eckardt⁴⁵, K.M. Ecker¹⁰³, R.C. Edgar⁹², T. Eifert³², G. Eigen¹⁵, K. Einsweiler¹⁶, T. Ekelof¹⁶⁸, M. El Kacimi^{137c}, V. Ellajosyula⁸⁸, M. Ellert¹⁶⁸, S. Elles⁵, F. Ellinghaus¹⁷⁸, A.A. Elliot¹⁷², N. Ellis³², J. Elmsheuser²⁷, M. Elsing³², D. Emeliyanov¹³³, Y. Enari¹⁵⁷, O.C. Endner⁸⁶, J.S. Ennis¹⁷³, J. Erdmann⁴⁶, A. Ereditato¹⁸, G. Ernis¹⁷⁸, M. Ernst²⁷, S. Errede¹⁶⁹, E. Ertel⁸⁶, M. Escalier¹¹⁹, H. Esch⁴⁶, C. Escobar¹²⁷, B. Esposito⁵⁰, A.I. Etienvre¹³⁸, E. Etzion¹⁵⁵, H. Evans⁶⁴, A. Ezhilov¹²⁵, M. Ezzi^{137e}, F. Fabbri^{22a,22b}, L. Fabbri^{22a,22b}, G. Facini³³, R.M. Fakhrutdinov¹³², S. Falciano^{134a}, R.J. Falla⁸¹, J. Faltova³², Y. Fang^{35a}, M. Fanti^{94a,94b}, A. Farbin⁸, A. Farilla^{136a}, C. Farina¹²⁷, E.M. Farina^{123a,123b}, T. Farooque⁹³, S. Farrell¹⁶, S.M. Farrington¹⁷³, P. Farthouat³², F. Fassi^{137e}, P. Fassnacht³², D. Fassouliotis⁹, M. Faucci Giannelli⁸⁰, A. Favaretto^{53a,53b}, W.J. Fawcett¹²², L. Fayard¹¹⁹, O.L. Fedin^{125,p}, W. Fedorko¹⁷¹, S. Feigl¹²¹, L. Feligioni⁸⁸, C. Feng^{36b}, E.J. Feng³², H. Feng⁹², A.B. Fenyuk¹³², L. Feremenga⁸, P. Fernandez Martinez¹⁷⁰, S. Fernandez Perez¹³, J. Ferrando⁴⁵, A. Ferrari¹⁶⁸, P. Ferrari¹⁰⁹, R. Ferrari^{123a}, D.E. Ferreira de Lima^{60b}, A. Ferrer¹⁷⁰, D. Ferrere⁵², C. Ferretti⁹², F. Fiedler⁸⁶, A. Filipčič⁷⁸, M. Filipuzzi⁴⁵, F. Filthaut¹⁰⁸, M. Fincke-Keeler¹⁷², K.D. Finelli¹⁵², M.C.N. Fiolhais^{128a,128c}, L. Fiorini¹⁷⁰, A. Fischer², C. Fischer¹³, J. Fischer¹⁷⁸, W.C. Fisher⁹³, N. Flaschel⁴⁵, I. Fleck¹⁴³, P. Fleischmann⁹², R.R.M. Fletcher¹²⁴, T. Flick¹⁷⁸, B.M. Flierl¹⁰², L.R. Flores Castillo^{62a}, M.J. Flowerdew¹⁰³, G.T. Forcolin⁸⁷, A. Formica¹³⁸, A. Forti⁸⁷, A.G. Foster¹⁹, D. Fournier¹¹⁹, H. Fox⁷⁵, S. Fracchia¹³, P. Francavilla⁸³, M. Franchini^{22a,22b}, D. Francis³², L. Franconi¹²¹, M. Franklin⁵⁹, M. Frate¹⁶⁶, M. Fraternali^{123a,123b}, D. Freeborn⁸¹, S.M. Fressard-Batraneanu³², B. Freund⁹⁷, D. Froidevaux³², J.A. Frost¹²², C. Fukunaga¹⁵⁸, E. Fullana Torregrossa⁸⁶, T. Fusayasu¹⁰⁴, J. Fuster¹⁷⁰, C. Gabaldon⁵⁸, O. Gabizon¹⁵⁴, A. Gabrielli^{22a,22b}, A. Gabrielli¹⁶, G.P. Gach^{41a}, S. Gadatsch³², S. Gadomski⁸⁰, G. Gagliardi^{53a,53b}, L.G. Gagnon⁹⁷,

P. Gagnon⁶⁴, C. Galea¹⁰⁸, B. Galhardo^{128a,128c}, E.J. Gallas¹²², B.J. Gallop¹³³, P. Gallus¹³⁰, G. Galster³⁹, K.K. Gan¹¹³, S. Ganguly³⁷, J. Gao^{36a}, Y. Gao⁷⁷, Y.S. Gao^{145,g}, F.M. Garay Walls⁴⁹, C. García¹⁷⁰, J.E. García Navarro¹⁷⁰, M. Garcia-Sciveres¹⁶, R.W. Gardner³³, N. Garelli¹⁴⁵, V. Garonne¹²¹, A. Gascon Bravo⁴⁵, K. Gasnikova⁴⁵, C. Gatti⁵⁰, A. Gaudiello^{53a,53b}, G. Gaudio^{123a}, I.L. Gavrilenko⁹⁸, C. Gay¹⁷¹, G. Gaycken²³, E.N. Gazis¹⁰, C.N.P. Gee¹³³, M. Geisen⁸⁶, M.P. Geisler^{60a}, K. Gellerstedt^{148a,148b}, C. Gemme^{53a}, M.H. Genest⁵⁸, C. Geng^{36a,q}, S. Gentile^{134a,134b}, C. Gentsos¹⁵⁶, S. George⁸⁰, D. Gerbaudo¹³, A. Gershon¹⁵⁵, S. Ghasemi¹⁴³, M. Ghneimat²³, B. Giacobbe^{22a}, S. Giagu^{134a,134b}, P. Giannetti^{126a,126b}, S.M. Gibson⁸⁰, M. Gignac¹⁷¹, M. Gilchriese¹⁶, D. Gillberg³¹, G. Gilles¹⁷⁸, D.M. Gingrich^{3,d}, N. Giokaris^{9,*}, M.P. Giordani^{167a,167c}, F.M. Giorgi^{22a}, P.F. Giraud¹³⁸, P. Giromini⁵⁹, D. Giugni^{94a}, F. Giulì¹²², C. Giuliani¹⁰³, M. Giulini^{60b}, B.K. Gjelsten¹²¹, S. Gkaitatzis¹⁵⁶, I. Gkialas⁹, E.L. Gkougkousis¹³⁹, L.K. Gladilin¹⁰¹, C. Glasman⁸⁵, J. Glatzer¹³, P.C.F. Glaysher⁴⁵, A. Glazov⁴⁵, M. Goblirsch-Kolb²⁵, J. Godlewski⁴², S. Goldfarb⁹¹, T. Golling⁵², D. Golubkov¹³², A. Gomes^{128a,128b,128d}, R. Gonçalo^{128a}, R. Goncalves Gama^{26a}, J. Goncalves Pinto Firmino Da Costa¹³⁸, G. Gonella⁵¹, L. Gonella¹⁹, A. Gongadze⁶⁸, S. González de la Hoz¹⁷⁰, S. Gonzalez-Sevilla⁵², L. Goossens³², P.A. Gorbounov⁹⁹, H.A. Gordon²⁷, I. Gorelov¹⁰⁷, B. Gorini³², E. Gorini^{76a,76b}, A. Gorišek⁷⁸, A.T. Goshaw⁴⁸, C. Gössling⁴⁶, M.I. Gostkin⁶⁸, C.R. Goudet¹¹⁹, D. Goujdami^{137c}, A.G. Goussiou¹⁴⁰, N. Govender^{147b,r}, E. Gozani¹⁵⁴, L. Gruber⁵⁷, I. Grabowska-Bold^{41a}, P.O.J. Gradin⁵⁸, J. Gramling⁵², E. Gramstad¹²¹, S. Grancagnolo¹⁷, V. Gratchev¹²⁵, P.M. Gravila^{28f}, H.M. Gray³², Z.D. Greenwood^{82,s}, C. Grefe²³, K. Gregersen⁸¹, I.M. Gregor⁴⁵, P. Grenier¹⁴⁵, K. Grevtsov⁵, J. Griffiths⁸, A.A. Grillo¹³⁹, K. Grimm⁷⁵, S. Grinstein^{13,t}, Ph. Gris³⁷, J.-F. Grivaz¹¹⁹, S. Groh⁸⁶, E. Gross¹⁷⁵, J. Grossé-Knetter⁵⁷, G.C. Grossi⁸², Z.J. Grout⁸¹, L. Guan⁹², W. Guan¹⁷⁶, J. Guenther⁶⁵, F. Guescini^{163a}, D. Guest¹⁶⁶, O. Gueta¹⁵⁵, B. Gui¹¹³, E. Guido^{53a,53b}, T. Guillemain⁵, S. Guindon², U. Gul⁵⁶, C. Gumpert³², J. Guo^{36c}, W. Guo⁹², Y. Guo^{36a}, R. Gupta⁴³, S. Gupta¹²², G. Gustavino^{134a,134b}, P. Gutierrez¹¹⁵, N.G. Gutierrez Ortiz⁸¹, C. Gutschow⁸¹, C. Guyot¹³⁸, M.P. Guzik^{41a}, C. Gwenlan¹²², C.B. Gwilliam⁷⁷, A. Haas¹¹², C. Haber¹⁶, H.K. Hadavand⁸, N. Haddad^{137e}, A. Hadef⁸⁸, S. Hageböck²³, M. Hagihara¹⁶⁴, H. Hakobyan^{180,*}, M. Haleem⁴⁵, J. Haley¹¹⁶, G. Halladjian⁹³, G.D. Hallewell⁸⁸, K. Hamacher¹⁷⁸, P. Hamal¹¹⁷, K. Hamano¹⁷², A. Hamilton^{147a}, G.N. Hamity¹⁴¹, P.G. Hamnett⁴⁵, L. Han^{36a}, S. Han^{35a}, K. Hanagaki^{69,u}, K. Hanawa¹⁵⁷, M. Hance¹³⁹, B. Haney¹²⁴, P. Hanke^{60a}, R. Hanna¹³⁸, J.B. Hansen³⁹, J.D. Hansen³⁹, M.C. Hansen²³, P.H. Hansen³⁹, K. Hara¹⁶⁴, A.S. Hard¹⁷⁶, T. Harenberg¹⁷⁸, F. Hariri¹¹⁹, S. Harkusha⁹⁵, R.D. Harrington⁴⁹, P.F. Harrison¹⁷³, F. Hartjes¹⁰⁹, N.M. Hartmann¹⁰², M. Hasegawa⁷⁰, Y. Hasegawa¹⁴², A. Hasib⁴⁹, S. Hassani¹³⁸, S. Haug¹⁸, R. Hauser⁹³, L. Hauswald⁴⁷, L.B. Havener³⁸, M. Havranek¹³⁰, C.M. Hawkes¹⁹, R.J. Hawkings³², D. Hayakawa¹⁵⁹, D. Hayden⁹³, C.P. Hays¹²², J.M. Hays⁷⁹, H.S. Hayward⁷⁷, S.J. Haywood¹³³, S.J. Head¹⁹, T. Heck⁸⁶, V. Hedberg⁸⁴, L. Heelan⁸, S. Heim⁴⁵, T. Heim¹⁶, B. Heinemann^{45,v}, J.J. Heinrich¹⁰², L. Heinrich¹¹², C. Heinz⁵⁵, J. Hejbal¹²⁹, L. Helary³², A. Held¹⁷¹, S. Hellman^{148a,148b}, C. Helsens³², J. Henderson¹²², R.C.W. Henderson⁷⁵, Y. Heng¹⁷⁶, S. Henkelmann¹⁷¹, A.M. Henriques Correia³², S. Henrot-Versille¹¹⁹, G.H. Herbert¹⁷, H. Herde²⁵, V. Herget¹⁷⁷, Y. Hernández Jiménez^{147c}, G. Herten⁵¹, R. Hertenberger¹⁰², L. Hervas³², T.C. Herwig¹²⁴, G.G. Hesketh⁸¹, N.P. Hessey¹⁰⁹, J.W. Hetherly⁴³, S. Higashino⁶⁹, E. Higón-Rodríguez¹⁷⁰, E. Hill¹⁷², J.C. Hill³⁰, K.H. Hiller⁴⁵, S.J. Hillier¹⁹, I. Hincliffe¹⁶, M. Hirose⁵¹, D. Hirschbuehl¹⁷⁸, B. Hiti⁷⁸, O. Hladík¹²⁹, X. Hoad⁴⁹, J. Hobbs¹⁵⁰, N. Hod^{163a}, M.C. Hodgkinson¹⁴¹, P. Hodgson¹⁴¹, A. Hoecker³², M.R. Hoeferkamp¹⁰⁷, F. Hoenig¹⁰², D. Hohn²³, T.R. Holmes¹⁶, M. Homann⁴⁶, S. Honda¹⁶⁴, T. Honda⁶⁹, T.M. Hong¹²⁷, B.H. Hooberman¹⁶⁹, W.H. Hopkins¹¹⁸, Y. Horii¹⁰⁵, A.J. Horton¹⁴⁴, J-Y. Hostachy⁵⁸, S. Hou¹⁵³, A. Hoummada^{137a}, J. Howarth⁴⁵, J. Hoya⁷⁴, M. Hrabovsky¹¹⁷, I. Hristova¹⁷, J. Hrvnac¹¹⁹, T. Hrynevich⁹⁶, P.J. Hsu⁶³, S.-C. Hsu¹⁴⁰, Q. Hu^{36a}, S. Hu^{36c}, Y. Huang^{35a}, Z. Hubacek¹³⁰, F. Hubaut⁸⁸, F. Huegging²³, T.B. Huffman¹²², E.W. Hughes³⁸, G. Hughes⁷⁵, M. Huhtinen³², P. Huo¹⁵⁰, N. Huseynov^{68,b}, J. Huston⁹³, J. Huth⁵⁹, G. Iacobucci⁵², G. Iakovidis²⁷, I. Ibragimov¹⁴³, L. Iconomidou-Fayard¹¹⁹, Z. Idrissi^{137e}, P. Iengo³²,

O. Igonkina^{109,w}, T. Iizawa¹⁷⁴, Y. Ikegami⁶⁹, M. Ikeno⁶⁹, Y. Ilchenko^{11,x}, D. Iliadis¹⁵⁶, N. Illic¹⁴⁵,
 G. Introzzi^{123a,123b}, P. Ioannou^{9,*}, M. Iodice^{136a}, K. Iordanidou³⁸, V. Ippolito⁵⁹, N. Ishijima¹²⁰,
 M. Ishino¹⁵⁷, M. Ishitsuka¹⁵⁹, C. Issever¹²², S. Isti^{20a}, F. Ito¹⁶⁴, J.M. Iturbe Ponce⁸⁷, R. Iuppa^{162a,162b},
 H. Iwasaki⁶⁹, J.M. Izen⁴⁴, V. Izzo^{106a}, S. Jabbar³, P. Jackson¹, V. Jain², K.B. Jakobi⁸⁶, K. Jakobs⁵¹,
 S. Jakobsen³², T. Jakoubek¹²⁹, D.O. Jamin¹¹⁶, D.K. Jana⁸², R. Jansky⁶⁵, J. Janssen²³, M. Janus⁵⁷,
 P.A. Janus^{41a}, G. Jarlskog⁸⁴, N. Javadov^{68,b}, T. Javůrek⁵¹, M. Javurkova⁵¹, F. Jeanneau¹³⁸, L. Jeanty¹⁶,
 J. Jejelava^{54a,y}, A. Jelinskas¹⁷³, P. Jenni^{51,z}, C. Jeske¹⁷³, S. Jézéquel⁵, H. Ji¹⁷⁶, J. Jia¹⁵⁰, H. Jiang⁶⁷,
 Y. Jiang^{36a}, Z. Jiang¹⁴⁵, S. Jiggins⁸¹, J. Jimenez Pena¹⁷⁰, S. Jin^{35a}, A. Jinaru^{28b}, O. Jinnouchi¹⁵⁹,
 H. Jivan^{147c}, P. Johansson¹⁴¹, K.A. Johns⁷, C.A. Johnson⁶⁴, W.J. Johnson¹⁴⁰, K. Jon-And^{148a,148b},
 R.W.L. Jones⁷⁵, S. Jones⁷, T.J. Jones⁷⁷, J. Jongmanns^{60a}, P.M. Jorge^{128a,128b}, J. Jovicevic^{163a}, X. Ju¹⁷⁶,
 A. Juste Rozas^{13,t}, M.K. Köhler¹⁷⁵, A. Kaczmarska⁴², M. Kado¹¹⁹, H. Kagan¹¹³, M. Kagan¹⁴⁵,
 S.J. Kahn⁸⁸, T. Kaji¹⁷⁴, E. Kajomovitz⁴⁸, C.W. Kalderon⁸⁴, A. Kaluza⁸⁶, S. Kama⁴³,
 A. Kamenshchikov¹³², N. Kanaya¹⁵⁷, S. Kaneti³⁰, L. Kanjir⁷⁸, V.A. Kantserov¹⁰⁰, J. Kanzaki⁶⁹,
 B. Kaplan¹¹², L.S. Kaplan¹⁷⁶, D. Kar^{147c}, K. Karakostas¹⁰, N. Karastathis¹⁰, M.J. Kareem⁵⁷,
 E. Karentzos¹⁰, S.N. Karpov⁶⁸, Z.M. Karpova⁶⁸, K. Karthik¹¹², V. Kartvelishvili⁷⁵, A.N. Karyukhin¹³²,
 K. Kasahara¹⁶⁴, L. Kashif¹⁷⁶, R.D. Kass¹¹³, A. Kastanas¹⁴⁹, Y. Kataoka¹⁵⁷, C. Kato¹⁵⁷, A. Katre⁵²,
 J. Katzy⁴⁵, K. Kawade¹⁰⁵, K. Kawagoe⁷³, T. Kawamoto¹⁵⁷, G. Kawamura⁵⁷, V.F. Kazanin^{111,c},
 R. Keeler¹⁷², R. Kehoe⁴³, J.S. Keller⁴⁵, J.J. Kempster⁸⁰, H. Keoshkerian¹⁶¹, O. Kepka¹²⁹,
 B.P. Kerševan⁷⁸, S. Kersten¹⁷⁸, R.A. Keyes⁹⁰, M. Khader¹⁶⁹, F. Khalil-zada¹², A. Khanov¹¹⁶,
 A.G. Kharlamov^{111,c}, T. Kharlamova^{111,c}, A. Khodinov¹⁶⁰, T.J. Khoo⁵², V. Khovanskiy⁹⁹,
 E. Khramov⁶⁸, J. Khubua^{54b,aa}, S. Kido⁷⁰, C.R. Kilby⁸⁰, H.Y. Kim⁸, S.H. Kim¹⁶⁴, Y.K. Kim³³,
 N. Kimura¹⁵⁶, O.M. Kind¹⁷, B.T. King⁷⁷, D. Kirchmeier⁴⁷, J. Kirk¹³³, A.E. Kiryunin¹⁰³,
 T. Kishimoto¹⁵⁷, D. Kisielewska^{41a}, K. Kiuchi¹⁶⁴, O. Kivernyk¹³⁸, E. Kladiva^{146b},
 T. Klapdor-kleingrothaus⁵¹, M.H. Klein³⁸, M. Klein⁷⁷, U. Klein⁷⁷, K. Kleinknecht⁸⁶, P. Klimek¹¹⁰,
 A. Klimentov²⁷, R. Klingenberg⁴⁶, T. Klioutchnikova³², E.-E. Kluge^{60a}, P. Kluit¹⁰⁹, S. Kluth¹⁰³,
 J. Knapik⁴², E. Knerner⁶⁵, E.B.F.G. Knoops⁸⁸, A. Knue¹⁰³, A. Kobayashi¹⁵⁷, D. Kobayashi¹⁵⁹,
 T. Kobayashi¹⁵⁷, M. Kobel⁴⁷, M. Kocian¹⁴⁵, P. Kodys¹³¹, T. Koffas³¹, E. Koffeman¹⁰⁹, N.M. Köhler¹⁰³,
 T. Koi¹⁴⁵, M. Kolb^{60b}, I. Koletsou⁵, A.A. Komar^{98,*}, Y. Komori¹⁵⁷, T. Kondo⁶⁹, N. Kondrashova^{36c},
 K. Köneke⁵¹, A.C. König¹⁰⁸, T. Kono^{69,ab}, R. Konoplich^{112,ac}, N. Konstantinidis⁸¹, R. Kopeliansky⁶⁴,
 S. Koperny^{41a}, A.K. Kopp⁵¹, K. Korcyl⁴², K. Kordas¹⁵⁶, A. Korn⁸¹, A.A. Korol^{111,c}, I. Korolkov¹³,
 E.V. Korolkova¹⁴¹, O. Kortner¹⁰³, S. Kortner¹⁰³, T. Kosek¹³¹, V.V. Kostyukhin²³, A. Kotwal⁴⁸,
 A. Koulouris¹⁰, A. Kourkoumeli-Charalampidi^{123a,123b}, C. Kourkoumelis⁹, V. Kouskoura²⁷,
 A.B. Kowalewska⁴², R. Kowalewski¹⁷², T.Z. Kowalski^{41a}, C. Kozakai¹⁵⁷, W. Kozanecki¹³⁸,
 A.S. Kozhin¹³², V.A. Kramarenko¹⁰¹, G. Kramberger⁷⁸, D. Krasnopalovtsev¹⁰⁰, M.W. Krasny⁸³,
 A. Krasznahorkay³², A. Kravchenko²⁷, J.A. Kremer^{41a}, M. Kretz^{60c}, J. Kretzschmar⁷⁷, K. Kreutzfeldt⁵⁵,
 P. Krieger¹⁶¹, K. Krizka³³, K. Kroeninger⁴⁶, H. Kroha¹⁰³, J. Kroll¹²⁴, J. Kroseberg²³, J. Krstic¹⁴,
 U. Kruchonak⁶⁸, H. Krüger²³, N. Krumnack⁶⁷, M.C. Kruse⁴⁸, M. Kruskal²⁴, T. Kubota⁹¹, H. Kucuk⁸¹,
 S. Kuday^{4b}, J.T. Kuechler¹⁷⁸, S. Kuehn⁵¹, A. Kugel^{60c}, F. Kuger¹⁷⁷, T. Kuhl⁴⁵, V. Kukhtin⁶⁸, R. Kukla⁸⁸,
 Y. Kulchitsky⁹⁵, S. Kuleshov^{34b}, Y.P. Kulinich¹⁶⁹, M. Kuna^{134a,134b}, T. Kunigo⁷¹, A. Kupco¹²⁹,
 O. Kuprash¹⁵⁵, H. Kurashige⁷⁰, L.L. Kurchaninov^{163a}, Y.A. Kurochkin⁹⁵, M.G. Kurth^{35a}, V. Kus¹²⁹,
 E.S. Kuwertz¹⁷², M. Kuze¹⁵⁹, J. Kvita¹¹⁷, T. Kwan¹⁷², D. Kyriazopoulos¹⁴¹, A. La Rosa¹⁰³,
 J.L. La Rosa Navarro^{26d}, L. La Rotonda^{40a,40b}, C. Lacasta¹⁷⁰, F. Lacava^{134a,134b}, J. Lacey⁴⁵, H. Lacker¹⁷,
 D. Lacour⁸³, E. Ladygin⁶⁸, R. Lafaye⁵, B. Laforge⁸³, T. Lagouri¹⁷⁹, S. Lai⁵⁷, S. Lammers⁶⁴, W. Lampl⁷,
 E. Lançon²⁷, U. Landgraf⁵¹, M.P.J. Landon⁷⁹, M.C. Lanfermann⁵², V.S. Lang^{60a}, J.C. Lange¹³,
 A.J. Lankford¹⁶⁶, F. Lanni²⁷, K. Lantzsch²³, A. Lanza^{123a}, A. Lapertosa^{53a,53b}, S. Laplace⁸³,
 J.F. Laporte¹³⁸, T. Lari^{94a}, F. Lasagni Manghi^{22a,22b}, M. Lassnig³², P. Laurelli⁵⁰, W. Lavrijzen¹⁶,
 A.T. Law¹³⁹, P. Laycock⁷⁷, T. Lazovich⁵⁹, M. Lazzaroni^{94a,94b}, B. Le⁹¹, O. Le Dortz⁸³, E. Le Guirriec⁸⁸,

E.P. Le Quilleuc¹³⁸, M. LeBlanc¹⁷², T. LeCompte⁶, F. Ledroit-Guillon⁵⁸, C.A. Lee²⁷, S.C. Lee¹⁵³,
 L. Lee¹, B. Lefebvre⁹⁰, G. Lefebvre⁸³, M. Lefebvre¹⁷², F. Legger¹⁰², C. Leggett¹⁶, A. Lehan⁷⁷,
 G. Lehmann Miotto³², X. Lei⁷, W.A. Leight⁴⁵, A.G. Leister¹⁷⁹, M.A.L. Leite^{26d}, R. Leitner¹³¹,
 D. Lellouch¹⁷⁵, B. Lemmer⁵⁷, K.J.C. Leney⁸¹, T. Lenz²³, B. Lenzi³², R. Leone⁷, S. Leone^{126a,126b},
 C. Leonidopoulos⁴⁹, G. Lerner¹⁵¹, C. Leroy⁹⁷, A.A.J. Lesage¹³⁸, C.G. Lester³⁰, M. Levchenko¹²⁵,
 J. Levêque⁵, D. Levin⁹², L.J. Levinson¹⁷⁵, M. Levy¹⁹, D. Lewis⁷⁹, M. Leyton⁴⁴, B. Li^{36a,q}, C. Li^{36a},
 H. Li¹⁵⁰, L. Li⁴⁸, L. Li^{36c}, Q. Li^{35a}, S. Li⁴⁸, X. Li^{36c}, Y. Li¹⁴³, Z. Liang^{35a}, B. Liberti^{135a}, A. Liblong¹⁶¹,
 K. Lie¹⁶⁹, J. Liebal²³, W. Liebig¹⁵, A. Limosani¹⁵², S.C. Lin^{153,ad}, T.H. Lin⁸⁶, B.E. Lindquist¹⁵⁰,
 A.E. Lioni⁵², E. Lipeles¹²⁴, A. Lipniacka¹⁵, M. Lisovyi^{60b}, T.M. Liss¹⁶⁹, A. Lister¹⁷¹, A.M. Litke¹³⁹,
 B. Liu^{153,ae}, H. Liu⁹², H. Liu²⁷, J. Liu^{36b}, J.B. Liu^{36a}, K. Liu⁸⁸, L. Liu¹⁶⁹, M. Liu^{36a}, Y.L. Liu^{36a},
 Y. Liu^{36a}, M. Livan^{123a,123b}, A. Lleres⁵⁸, J. Llorente Merino^{35a}, S.L. Lloyd⁷⁹, C.Y. Lo^{62b},
 F. Lo Sterzo¹⁵³, E.M. Lobodzinska⁴⁵, P. Loch⁷, F.K. Loebinger⁸⁷, K.M. Loew²⁵, A. Loginov^{179,*},
 T. Lohse¹⁷, K. Lohwasser⁴⁵, M. Lokajicek¹²⁹, B.A. Long²⁴, J.D. Long¹⁶⁹, R.E. Long⁷⁵, L. Longo^{76a,76b},
 K.A.Looper¹¹³, J.A. Lopez^{34b}, D. Lopez Mateos⁵⁹, I. Lopez Paz¹³, A. Lopez Solis⁸³, J. Lorenz¹⁰²,
 N. Lorenzo Martinez⁶⁴, M. Losada²¹, P.J. Lösel¹⁰², X. Lou^{35a}, A. Louinis¹¹⁹, J. Love⁶, P.A. Love⁷⁵,
 H. Lu^{62a}, N. Lu⁹², Y. Lu⁶³, H.J. Lubatti¹⁴⁰, C. Luci^{134a,134b}, A. Lucotte⁵⁸, C. Luedtke⁵¹, F. Luehring⁶⁴,
 W. Lukas⁶⁵, L. Luminari^{134a}, O. Lundberg^{148a,148b}, B. Lund-Jensen¹⁴⁹, P.M. Luzi⁸³, D. Lynn²⁷,
 R. Lysak¹²⁹, E. Lytken⁸⁴, V. Lyubushkin⁶⁸, H. Ma²⁷, L.L. Ma^{36b}, Y. Ma^{36b}, G. Maccarone⁵⁰,
 A. Macchiolo¹⁰³, C.M. Macdonald¹⁴¹, B. Maček⁷⁸, J. Machado Miguens^{124,128b}, D. Madaffari⁸⁸,
 R. Madar³⁷, H.J. Maddocks¹⁶⁸, W.F. Mader⁴⁷, A. Madsen⁴⁵, J. Maeda⁷⁰, S. Maeland¹⁵, T. Maeno²⁷,
 A. Maevskiy¹⁰¹, E. Magradze⁵⁷, J. Mahlstedt¹⁰⁹, C. Maiani¹¹⁹, C. Maidantchik^{26a}, A.A. Maier¹⁰³,
 T. Maier¹⁰², A. Maio^{128a,128b,128d}, S. Majewski¹¹⁸, Y. Makida⁶⁹, N. Makovec¹¹⁹, B. Malaescu⁸³,
 Pa. Malecki⁴², V.P. Maleev¹²⁵, F. Malek⁵⁸, U. Mallik⁶⁶, D. Malon⁶, C. Malone³⁰, S. Maltezos¹⁰,
 S. Malyukov³², J. Mamuzic¹⁷⁰, G. Mancini⁵⁰, L. Mandelli^{94a}, I. Mandić⁷⁸, J. Maneira^{128a,128b},
 L. Manhaes de Andrade Filho^{26b}, J. Manjarres Ramos^{163b}, A. Mann¹⁰², A. Manousos³²,
 B. Mansoulie¹³⁸, J.D. Mansour^{35a}, R. Mantifel⁹⁰, M. Mantoani⁵⁷, S. Manzoni^{94a,94b}, L. Mapelli³²,
 G. Marceca²⁹, L. March⁵², G. Marchiori⁸³, M. Marcisovsky¹²⁹, M. Marjanovic³⁷, D.E. Marley⁹²,
 F. Marroquim^{26a}, S.P. Marsden⁸⁷, Z. Marshall¹⁶, M.U.F Martensson¹⁶⁸, S. Marti-Garcia¹⁷⁰,
 C.B. Martin¹¹³, T.A. Martin¹⁷³, V.J. Martin⁴⁹, B. Martin dit Latour¹⁵, M. Martinez^{13,t},
 V.I. Martinez Outschoorn¹⁶⁹, S. Martin-Haugh¹³³, V.S. Martoiu^{28b}, A.C. Martyniuk⁸¹, A. Marzin¹¹⁵,
 L. Masetti⁸⁶, T. Mashimo¹⁵⁷, R. Mashinistov⁹⁸, J. Masik⁸⁷, A.L. Maslennikov^{111,c}, L. Massa^{135a,135b},
 P. Mastrandrea⁵, A. Mastroberardino^{40a,40b}, T. Masubuchi¹⁵⁷, P. Mättig¹⁷⁸, J. Maurer^{28b}, S.J. Maxfield⁷⁷,
 D.A. Maximov^{111,c}, R. Mazini¹⁵³, I. Maznas¹⁵⁶, S.M. Mazza^{94a,94b}, N.C. Mc Fadden¹⁰⁷,
 G. Mc Goldrick¹⁶¹, S.P. Mc Kee⁹², A. McCarn⁹², R.L. McCarthy¹⁵⁰, T.G. McCarthy¹⁰³,
 L.I. McClymont⁸¹, E.F. McDonald⁹¹, J.A. McFayden⁸¹, G. Mchedlidze⁵⁷, S.J. McMahon¹³³,
 P.C. McNamara⁹¹, R.A. McPherson^{172,n}, S. Meehan¹⁴⁰, T.J. Megy⁵¹, S. Mehlhase¹⁰², A. Mehta⁷⁷,
 T. Meideck⁵⁸, K. Meier^{60a}, C. Meineck¹⁰², B. Meirose⁴⁴, D. Melini^{170,af}, B.R. Mellado Garcia^{147c},
 M. Melo^{146a}, F. Meloni¹⁸, S.B. Menary⁸⁷, L. Meng⁷⁷, X.T. Meng⁹², A. Mengarelli^{22a,22b}, S. Menke¹⁰³,
 E. Meoni¹⁶⁵, S. Mergelmeyer¹⁷, P. Mermod⁵², L. Merola^{106a,106b}, C. Meroni^{94a}, F.S. Merritt³³,
 A. Messina^{134a,134b}, J. Metcalfe⁶, A.S. Mete¹⁶⁶, C. Meyer¹²⁴, J.-P. Meyer¹³⁸, J. Meyer¹⁰⁹,
 H. Meyer Zu Theenhausen^{60a}, F. Miano¹⁵¹, R.P. Middleton¹³³, S. Miglioranzi^{53a,53b}, L. Mijović⁴⁹,
 G. Mikenberg¹⁷⁵, M. Mikestikova¹²⁹, M. Mikuž⁷⁸, M. Milesi⁹¹, A. Milic²⁷, D.W. Miller³³, C. Mills⁴⁹,
 A. Milov¹⁷⁵, D.A. Milstead^{148a,148b}, A.A. Minaenko¹³², Y. Minami¹⁵⁷, I.A. Minashvili⁶⁸, A.I. Mincer¹¹²,
 B. Mindur^{41a}, M. Mineev⁶⁸, Y. Minegishi¹⁵⁷, Y. Ming¹⁷⁶, L.M. Mir¹³, K.P. Mistry¹²⁴, T. Mitani¹⁷⁴,
 J. Mitrevski¹⁰², V.A. Mitsou¹⁷⁰, A. Miucci¹⁸, P.S. Miyagawa¹⁴¹, A. Mizukami⁶⁹, J.U. Mjörnmark⁸⁴,
 M. Mlynarikova¹³¹, T. Moa^{148a,148b}, K. Mochizuki⁹⁷, P. Mogg⁵¹, S. Mohapatra³⁸, S. Molander^{148a,148b},
 R. Moles-Valls²³, R. Monden⁷¹, M.C. Mondragon⁹³, K. Möning⁴⁵, J. Monk³⁹, E. Monnier⁸⁸,

A. Montalbano¹⁵⁰, J. Montejo Berlingen³², F. Monticelli⁷⁴, S. Monzani^{94a,94b}, R.W. Moore³,
 N. Morange¹¹⁹, D. Moreno²¹, M. Moreno Llácer⁵⁷, P. Morettini^{53a}, S. Morgenstern³², D. Mori¹⁴⁴,
 T. Mori¹⁵⁷, M. Morii⁵⁹, M. Morinaga¹⁵⁷, V. Morisbak¹²¹, A.K. Morley¹⁵², G. Mornacchi³²,
 J.D. Morris⁷⁹, L. Morvaj¹⁵⁰, P. Moschovakos¹⁰, M. Mosidze^{54b}, H.J. Moss¹⁴¹, J. Moss^{145,ag},
 K. Motohashi¹⁵⁹, R. Mount¹⁴⁵, E. Mountricha²⁷, E.J.W. Moyse⁸⁹, S. Muanza⁸⁸, R.D. Mudd¹⁹,
 F. Mueller¹⁰³, J. Mueller¹²⁷, R.S.P. Mueller¹⁰², D. Muenstermann⁷⁵, P. Mullen⁵⁶, G.A. Mullier¹⁸,
 F.J. Munoz Sanchez⁸⁷, W.J. Murray^{173,133}, H. Musheghyan⁵⁷, M. Muškinja⁷⁸, A.G. Myagkov^{132,ah},
 M. Myska¹³⁰, B.P. Nachman¹⁶, O. Nackenhorst⁵², K. Nagai¹²², R. Nagai^{69,ab}, K. Nagano⁶⁹,
 Y. Nagasaka⁶¹, K. Nagata¹⁶⁴, M. Nagel⁵¹, E. Nagy⁸⁸, A.M. Nairz³², Y. Nakahama¹⁰⁵, K. Nakamura⁶⁹,
 T. Nakamura¹⁵⁷, I. Nakano¹¹⁴, R.F. Naranjo Garcia⁴⁵, R. Narayan¹¹, D.I. Narrias Villar^{60a},
 I. Naryshkin¹²⁵, T. Naumann⁴⁵, G. Navarro²¹, R. Nayyar⁷, H.A. Neal⁹², P.Yu. Nechaeva⁹⁸, T.J. Neep¹³⁸,
 A. Negri^{123a,123b}, M. Negrini^{22a}, S. Nektarijevic¹⁰⁸, C. Nellist¹¹⁹, A. Nelson¹⁶⁶, S. Nemecek¹²⁹,
 P. Nemethy¹¹², A.A. Nepomuceno^{26a}, M. Nessi^{32,ai}, M.S. Neubauer¹⁶⁹, M. Neumann¹⁷⁸, R.M. Neves¹¹²,
 P. Nevski²⁷, P.R. Newman¹⁹, T.Y. Ng^{62c}, T. Nguyen Manh⁹⁷, R.B. Nickerson¹²², R. Nicolaidou¹³⁸,
 J. Nielsen¹³⁹, V. Nikolaenko^{132,ah}, I. Nikolic-Audit⁸³, K. Nikolopoulos¹⁹, J.K. Nilsen¹²¹, P. Nilsson²⁷,
 Y. Ninomiya¹⁵⁷, A. Nisati^{134a}, N. Nishu^{35c}, R. Nisius¹⁰³, T. Nobe¹⁵⁷, Y. Noguchi⁷¹, M. Nomachi¹²⁰,
 I. Nomidis³¹, M.A. Nomura²⁷, T. Nooney⁷⁹, M. Nordberg³², N. Norjoharuddeen¹²², O. Novgorodova⁴⁷,
 S. Nowak¹⁰³, M. Nozaki⁶⁹, L. Nozka¹¹⁷, K. Ntekas¹⁶⁶, E. Nurse⁸¹, F. Nuti⁹¹, D.C. O'Neil¹⁴⁴,
 A.A. O'Rourke⁴⁵, V. O'Shea⁵⁶, F.G. Oakham^{31,d}, H. Oberlack¹⁰³, T. Obermann²³, J. Ocariz⁸³,
 A. Ochi⁷⁰, I. Ochoa³⁸, J.P. Ochoa-Ricoux^{34a}, S. Oda⁷³, S. Odaka⁶⁹, H. Ogren⁶⁴, A. Oh⁸⁷, S.H. Oh⁴⁸,
 C.C. Ohm¹⁶, H. Ohman¹⁶⁸, H. Oide^{53a,53b}, H. Okawa¹⁶⁴, Y. Okumura¹⁵⁷, T. Okuyama⁶⁹, A. Olariu^{28b},
 L.F. Oleiro Seabra^{128a}, S.A. Olivares Pino⁴⁹, D. Oliveira Damazio²⁷, A. Olszewski⁴², J. Olszowska⁴²,
 A. Onofre^{128a,128e}, K. Onogi¹⁰⁵, P.U.E. Onyisi^{11,x}, M.J. Oreglia³³, Y. Oren¹⁵⁵, D. Orestano^{136a,136b},
 N. Orlando^{62b}, R.S. Orr¹⁶¹, B. Osculati^{53a,53b,*}, R. Ospanov⁸⁷, G. Otero y Garzon²⁹, H. Otono⁷³,
 M. Ouchrif^{137d}, F. Ould-Saada¹²¹, A. Ouraou¹³⁸, K.P. Oussoren¹⁰⁹, Q. Ouyang^{35a}, M. Owen⁵⁶,
 R.E. Owen¹⁹, V.E. Ozcan^{20a}, N. Ozturk⁸, K. Pachal¹⁴⁴, A. Pacheco Pages¹³, L. Pacheco Rodriguez¹³⁸,
 C. Padilla Aranda¹³, S. Pagan Griso¹⁶, M. Paganini¹⁷⁹, F. Paige²⁷, P. Pais⁸⁹, G. Palacino⁶⁴,
 S. Palazzo^{40a,40b}, S. Palestini³², M. Palka^{41b}, D. Pallin³⁷, E.St. Panagiotopoulou¹⁰, I. Panagoulias¹⁰,
 C.E. Pandini⁸³, J.G. Panduro Vazquez⁸⁰, P. Pani³², S. Panitkin²⁷, D. Pantea^{28b}, L. Paolozzi⁵²,
 Th.D. Papadopoulou¹⁰, K. Papageorgiou⁹, A. Paramonov⁶, D. Paredes Hernandez¹⁷⁹, A.J. Parker⁷⁵,
 M.A. Parker³⁰, K.A. Parker⁴⁵, F. Parodi^{53a,53b}, J.A. Parsons³⁸, U. Parzefall⁵¹, V.R. Pascuzzi¹⁶¹,
 J.M. Pasner¹³⁹, E. Pasqualucci^{134a}, S. Passaggio^{53a}, Fr. Pastore⁸⁰, S. Pataraia¹⁷⁸, J.R. Pater⁸⁷, T. Pauly³²,
 J. Pearce¹⁷², B. Pearson¹¹⁵, L.E. Pedersen³⁹, S. Pedraza Lopez¹⁷⁰, R. Pedro^{128a,128b},
 S.V. Peleganchuk^{111,c}, O. Penc¹²⁹, C. Peng^{35a}, H. Peng^{36a}, J. Penwell⁶⁴, B.S. Peralva^{26b},
 M.M. Pereo¹³⁸, D.V. Perepelitsa²⁷, L. Perini^{94a,94b}, H. Pernegger³², S. Perrella^{106a,106b}, R. Peschke⁴⁵,
 V.D. Peshekhonov⁶⁸, K. Peters⁴⁵, R.F.Y. Peters⁸⁷, B.A. Petersen³², T.C. Petersen³⁹, E. Petit⁵⁸,
 A. Petridis¹, C. Petridou¹⁵⁶, P. Petroff¹¹⁹, E. Petrolo^{134a}, M. Petrov¹²², F. Petracci^{136a,136b},
 N.E. Pettersson⁸⁹, A. Peyaud¹³⁸, R. Pezoa^{34b}, P.W. Phillips¹³³, G. Piacquadio¹⁵⁰, E. Pianori¹⁷³,
 A. Picazio⁸⁹, E. Piccaro⁷⁹, M.A. Pickering¹²², R. Piegaia²⁹, J.E. Pilcher³³, A.D. Pilkington⁸⁷,
 A.W.J. Pin⁸⁷, M. Pinamonti^{167a,167c,aj}, J.L. Pinfold³, H. Pirumov⁴⁵, M. Pitt¹⁷⁵, L. Plazak^{146a},
 M.-A. Pleier²⁷, V. Pleskot⁸⁶, E. Plotnikova⁶⁸, D. Pluth⁶⁷, P. Podbereko¹¹¹, R. Poettgen^{148a,148b},
 L. Poggioli¹¹⁹, D. Pohl²³, G. Polesello^{123a}, A. Poley⁴⁵, A. Pollicchio^{40a,40b}, R. Polifka³², A. Polini^{22a},
 C.S. Pollard⁵⁶, V. Polychronakos²⁷, K. Pommès³², L. Pontecorvo^{134a}, B.G. Pope⁹³, G.A. Popeneciu^{28d},
 A. Poppleton³², S. Pospisil¹³⁰, K. Potamianos¹⁶, I.N. Potrap⁶⁸, C.J. Potter³⁰, C.T. Potter¹¹⁸,
 G. Poulard³², J. Poveda³², M.E. Pozo Astigarraga³², P. Pralavorio⁸⁸, A. Pranko¹⁶, S. Prell⁶⁷, D. Price⁸⁷,
 L.E. Price⁶, M. Primavera^{76a}, S. Prince⁹⁰, K. Prokofiev^{62c}, F. Prokoshin^{34b}, S. Protopopescu²⁷,
 J. Proudfoot⁶, M. Przybycien^{41a}, D. Puddu^{136a,136b}, A. Puri¹⁶⁹, P. Puzo¹¹⁹, J. Qian⁹², G. Qin⁵⁶, Y. Qin⁸⁷,

A. Quadt⁵⁷, W.B. Quayle^{167a,167b}, M. Queitsch-Maitland⁴⁵, D. Quilty⁵⁶, S. Raddum¹²¹, V. Radeka²⁷, V. Radescu¹²², S.K. Radhakrishnan¹⁵⁰, P. Radloff¹¹⁸, P. Rados⁹¹, F. Ragusa^{94a,94b}, G. Rahal¹⁸¹, J.A. Raine⁸⁷, S. Rajagopalan²⁷, C. Rangel-Smith¹⁶⁸, M.G. Ratti^{94a,94b}, D.M. Rauch⁴⁵, F. Rauscher¹⁰², S. Rave⁸⁶, T. Ravenscroft⁵⁶, I. Ravinovich¹⁷⁵, M. Raymond³², A.L. Read¹²¹, N.P. Readioff⁷⁷, M. Reale^{76a,76b}, D.M. Rebuzzi^{123a,123b}, A. Redelbach¹⁷⁷, G. Redlinger²⁷, R. Reece¹³⁹, R.G. Reed^{147c}, K. Reeves⁴⁴, L. Rehnisch¹⁷, J. Reichert¹²⁴, A. Reiss⁸⁶, C. Rembser³², H. Ren^{35a}, M. Rescigno^{134a}, S. Resconi^{94a}, E.D. Resseguei¹²⁴, S. Rettie¹⁷¹, E. Reynolds¹⁹, O.L. Rezanova^{111,c}, P. Reznicek¹³¹, R. Rezvani⁹⁷, R. Richter¹⁰³, S. Richter⁸¹, E. Richter-Was^{41b}, O. Ricken²³, M. Ridel⁸³, P. Rieck¹⁰³, C.J. Riegel¹⁷⁸, J. Rieger⁵⁷, O. Rifki¹¹⁵, M. Rijssenbeek¹⁵⁰, A. Rimoldi^{123a,123b}, M. Rimoldi¹⁸, L. Rinaldi^{22a}, B. Ristic⁵², E. Ritsch³², I. Riu¹³, F. Rizatdinova¹¹⁶, E. Rizvi⁷⁹, C. Rizzi¹³, R.T. Roberts⁸⁷, S.H. Robertson^{90,n}, A. Robichaud-Veronneau⁹⁰, D. Robinson³⁰, J.E.M. Robinson⁴⁵, A. Robson⁵⁶, C. Roda^{126a,126b}, Y. Rodina^{88,ak}, A. Rodriguez Perez¹³, D. Rodriguez Rodriguez¹⁷⁰, S. Roe³², C.S. Rogan⁵⁹, O. Røhne¹²¹, J. Roloff⁵⁹, A. Romaniouk¹⁰⁰, M. Romano^{22a,22b}, S.M. Romano Saez³⁷, E. Romero Adam¹⁷⁰, N. Rompotis⁷⁷, M. Ronzani⁵¹, L. Roos⁸³, S. Rosati^{134a}, K. Rosbach⁵¹, P. Rose¹³⁹, N.-A. Rosien⁵⁷, V. Rossetti^{148a,148b}, E. Rossi^{106a,106b}, L.P. Rossi^{53a}, J.H.N. Rosten³⁰, R. Rosten¹⁴⁰, M. Rotaru^{28b}, I. Roth¹⁷⁵, J. Rothberg¹⁴⁰, D. Rousseau¹¹⁹, A. Rozanov⁸⁸, Y. Rozen¹⁵⁴, X. Ruan^{147c}, F. Rubbo¹⁴⁵, F. Rühr⁵¹, A. Ruiz-Martinez³¹, Z. Rurikova⁵¹, N.A. Rusakovich⁶⁸, A. Ruschke¹⁰², H.L. Russell¹⁴⁰, J.P. Rutherford⁷, N. Ruthmann³², Y.F. Ryabov¹²⁵, M. Rybar¹⁶⁹, G. Rybkin¹¹⁹, S. Ryu⁶, A. Ryzhov¹³², G.F. Rzehorz⁵⁷, A.F. Saavedra¹⁵², G. Sabato¹⁰⁹, S. Sacerdoti²⁹, H.F-W. Sadrozinski¹³⁹, R. Sadykov⁶⁸, F. Safai Tehrani^{134a}, P. Saha¹¹⁰, M. Sahinsoy^{60a}, M. Saimpert⁴⁵, T. Saito¹⁵⁷, H. Sakamoto¹⁵⁷, Y. Sakurai¹⁷⁴, G. Salamanna^{136a,136b}, J.E. Salazar Loyola^{34b}, D. Salek¹⁰⁹, P.H. Sales De Bruin¹⁴⁰, D. Salihagic¹⁰³, A. Salnikov¹⁴⁵, J. Salt¹⁷⁰, D. Salvatore^{40a,40b}, F. Salvatore¹⁵¹, A. Salvucci^{62a,62b,62c}, A. Salzburger³², D. Sammel⁵¹, D. Sampsonidis¹⁵⁶, J. Sánchez¹⁷⁰, V. Sanchez Martinez¹⁷⁰, A. Sanchez Pineda^{106a,106b}, H. Sandaker¹²¹, R.L. Sandbach⁷⁹, C.O. Sander⁴⁵, M. Sandhoff¹⁷⁸, C. Sandoval²¹, D.P.C. Sankey¹³³, M. Sannino^{53a,53b}, A. Sansoni⁵⁰, C. Santoni³⁷, R. Santonico^{135a,135b}, H. Santos^{128a}, I. Santoyo Castillo¹⁵¹, K. Sapp¹²⁷, A. Sapronov⁶⁸, J.G. Saraiva^{128a,128d}, B. Sarrazin²³, O. Sasaki⁶⁹, K. Sato¹⁶⁴, E. Sauvan⁵, G. Savage⁸⁰, P. Savard^{161,d}, N. Savic¹⁰³, C. Sawyer¹³³, L. Sawyer^{82,s}, J. Saxon³³, C. Sbarra^{22a}, A. Sbrizzi^{22a,22b}, T. Scanlon⁸¹, D.A. Scannicchio¹⁶⁶, M. Scarcella¹⁵², V. Scarfone^{40a,40b}, J. Schaarschmidt¹⁴⁰, P. Schacht¹⁰³, B.M. Schachtner¹⁰², D. Schaefer³², L. Schaefer¹²⁴, R. Schaefer⁴⁵, J. Schaeffer⁸⁶, S. Schaepe²³, S. Schaetzl^{60b}, U. Schäfer⁸⁶, A.C. Schaffer¹¹⁹, D. Schaile¹⁰², R.D. Schamberger¹⁵⁰, V. Scharf^{60a}, V.A. Schegelsky¹²⁵, D. Scheirich¹³¹, M. Schernau¹⁶⁶, C. Schiavi^{53a,53b}, S. Schier¹³⁹, C. Schillo⁵¹, M. Schioppa^{40a,40b}, S. Schlenker³², K.R. Schmidt-Sommerfeld¹⁰³, K. Schmieden³², C. Schmitt⁸⁶, S. Schmitt⁴⁵, S. Schmitz⁸⁶, B. Schneider^{163a}, U. Schnoor⁵¹, L. Schoeffel¹³⁸, A. Schoening^{60b}, B.D. Schoenrock⁹³, E. Schopf²³, M. Schott⁸⁶, J.F.P. Schouwenberg¹⁰⁸, J. Schovancova⁸, S. Schramm⁵², N. Schuh⁸⁶, A. Schulte⁸⁶, M.J. Schultens²³, H.-C. Schultz-Coulon^{60a}, H. Schulz¹⁷, M. Schumacher⁵¹, B.A. Schumm¹³⁹, Ph. Schune¹³⁸, A. Schwartzman¹⁴⁵, T.A. Schwarz⁹², H. Schweiger⁸⁷, Ph. Schwemling¹³⁸, R. Schwienhorst⁹³, J. Schwindling¹³⁸, T. Schwindt²³, G. Sciolla²⁵, F. Scuri^{126a,126b}, F. Scutti⁹¹, J. Searcy⁹², P. Seema²³, S.C. Seidel¹⁰⁷, A. Seiden¹³⁹, J.M. Seixas^{26a}, G. Sekhniaidze^{106a}, K. Sekhon⁹², S.J. Sekula⁴³, N. Semprini-Cesari^{22a,22b}, C. Serfon¹²¹, L. Serin¹¹⁹, L. Serkin^{167a,167b}, M. Sessa^{136a,136b}, R. Seuster¹⁷², H. Severini¹¹⁵, T. Sfiligoj⁷⁸, F. Sforza³², A. Sfyrla⁵², E. Shabalina⁵⁷, N.W. Shaikh^{148a,148b}, L.Y. Shan^{35a}, R. Shang¹⁶⁹, J.T. Shank²⁴, M. Shapiro¹⁶, P.B. Shatalov⁹⁹, K. Shaw^{167a,167b}, S.M. Shaw⁸⁷, A. Shcherbakova^{148a,148b}, C.Y. Shehu¹⁵¹, Y. Shen¹¹⁵, P. Sherwood⁸¹, L. Shi^{153,al}, S. Shimizu⁷⁰, C.O. Shimmin¹⁶⁶, M. Shimojima¹⁰⁴, S. Shirabe⁷³, M. Shiyakova^{68,am}, J. Shlomi¹⁷⁵, A. Shmeleva⁹⁸, D. Shoaleh Saadi⁹⁷, M.J. Shochet³³, S. Shojaii^{94a}, D.R. Shope¹¹⁵, S. Shrestha¹¹³, E. Shulga¹⁰⁰, M.A. Shupe⁷, P. Sicho¹²⁹, A.M. Sickles¹⁶⁹, P.E. Sidebo¹⁴⁹, E. Sideras Haddad^{147c}, O. Sidiropoulou¹⁷⁷, D. Sidorov¹¹⁶, A. Sidoti^{22a,22b}, F. Siegert⁴⁷, Dj. Sijacki¹⁴,

J. Silva^{128a,128d}, S.B. Silverstein^{148a}, V. Simak¹³⁰, Lj. Simic¹⁴, S. Simion¹¹⁹, E. Simioni⁸⁶,
 B. Simmons⁸¹, M. Simon⁸⁶, P. Sinervo¹⁶¹, N.B. Sinev¹¹⁸, M. Sioli^{22a,22b}, G. Siragusa¹⁷⁷, I. Siral⁹²,
 S.Yu. Sivoklokov¹⁰¹, J. Sjölin^{148a,148b}, M.B. Skinner⁷⁵, P. Skubic¹¹⁵, M. Slater¹⁹, T. Slavicek¹³⁰,
 M. Slawinska¹⁰⁹, K. Sliwa¹⁶⁵, R. Slovak¹³¹, V. Smakhtin¹⁷⁵, B.H. Smart⁵, L. Smestad¹⁵, J. Smiesko^{146a},
 S.Yu. Smirnov¹⁰⁰, Y. Smirnov¹⁰⁰, L.N. Smirnova^{101,an}, O. Smirnova⁸⁴, J.W. Smith⁵⁷, M.N.K. Smith³⁸,
 R.W. Smith³⁸, M. Smizanska⁷⁵, K. Smolek¹³⁰, A.A. Snesarev⁹⁸, I.M. Snyder¹¹⁸, S. Snyder²⁷,
 R. Sobie^{172,n}, F. Socher⁴⁷, A. Soffer¹⁵⁵, D.A. Soh¹⁵³, G. Sokhrannyi⁷⁸, C.A. Solans Sanchez³²,
 M. Solar¹³⁰, E.Yu. Soldatov¹⁰⁰, U. Soldevila¹⁷⁰, A.A. Solodkov¹³², A. Soloshenko⁶⁸,
 O.V. Solovyanov¹³², V. Solovyev¹²⁵, P. Sommer⁵¹, H. Son¹⁶⁵, H.Y. Song^{36a,ao}, A. Sopczak¹³⁰,
 V. Sorin¹³, D. Sosa^{60b}, C.L. Sotiropoulou^{126a,126b}, R. Soualah^{167a,167c}, A.M. Soukharev^{111,c}, D. South⁴⁵,
 B.C. Sowden⁸⁰, S. Spagnolo^{76a,76b}, M. Spalla^{126a,126b}, M. Spangenberg¹⁷³, F. Spanò⁸⁰, D. Sperlich¹⁷,
 F. Spettel¹⁰³, T.M. Spieker^{60a}, R. Spighi^{22a}, G. Spigo³², L.A. Spiller⁹¹, M. Spousta¹³¹, R.D. St. Denis^{56,*},
 A. Stabile^{94a}, R. Stamen^{60a}, S. Stamm¹⁷, E. Stanecka⁴², R.W. Stanek⁶, C. Stanescu^{136a},
 M.M. Stanitzki⁴⁵, S. Stapnes¹²¹, E.A. Starchenko¹³², G.H. Stark³³, J. Stark⁵⁸, S.H Stark³⁹, P. Staroba¹²⁹,
 P. Starovoitov^{60a}, S. Stärz³², R. Staszewski⁴², P. Steinberg²⁷, B. Stelzer¹⁴⁴, H.J. Stelzer³²,
 O. Stelzer-Chilton^{163a}, H. Stenzel⁵⁵, G.A. Stewart⁵⁶, J.A. Stillings²³, M.C. Stockton⁹⁰, M. Stoebe⁹⁰,
 G. Stoica^{28b}, P. Stolte⁵⁷, S. Stonjek¹⁰³, A.R. Stradling⁸, A. Straessner⁴⁷, M.E. Stramaglia¹⁸,
 J. Strandberg¹⁴⁹, S. Strandberg^{148a,148b}, A. Strandlie¹²¹, M. Strauss¹¹⁵, P. Strizenec^{146b}, R. Ströhmer¹⁷⁷,
 D.M. Strom¹¹⁸, R. Stroynowski⁴³, A. Strubig¹⁰⁸, S.A. Stucci²⁷, B. Stugu¹⁵, N.A. Styles⁴⁵, D. Su¹⁴⁵,
 J. Su¹²⁷, S. Suchek^{60a}, Y. Sugaya¹²⁰, M. Suk¹³⁰, V.V. Sulin⁹⁸, S. Sultansoy^{4c}, T. Sumida⁷¹, S. Sun⁵⁹,
 X. Sun³, K. Suruliz¹⁵¹, C.J.E. Suster¹⁵², M.R. Sutton¹⁵¹, S. Suzuki⁶⁹, M. Svatos¹²⁹, M. Swiatlowski³³,
 S.P. Swift², I. Sykora^{146a}, T. Sykora¹³¹, D. Ta⁵¹, K. Tackmann⁴⁵, J. Taenzer¹⁵⁵, A. Taffard¹⁶⁶,
 R. Tafirout^{163a}, N. Taiblum¹⁵⁵, H. Takai²⁷, R. Takashima⁷², T. Takeshita¹⁴², Y. Takubo⁶⁹, M. Talby⁸⁸,
 A.A. Talyshев^{111,c}, J. Tanaka¹⁵⁷, M. Tanaka¹⁵⁹, R. Tanaka¹¹⁹, S. Tanaka⁶⁹, R. Tanioka⁷⁰,
 B.B. Tannenwald¹¹³, S. Tapia Araya^{34b}, S. Tapprogge⁸⁶, S. Tarem¹⁵⁴, G.F. Tartarelli^{94a}, P. Tas¹³¹,
 M. Tasevsky¹²⁹, T. Tashiro⁷¹, E. Tassi^{40a,40b}, A. Tavares Delgado^{128a,128b}, Y. Tayalati^{137e}, A.C. Taylor¹⁰⁷,
 G.N. Taylor⁹¹, P.T.E. Taylor⁹¹, W. Taylor^{163b}, P. Teixeira-Dias⁸⁰, K.K. Temming⁵¹, D. Temple¹⁴⁴,
 H. Ten Kate³², P.K. Teng¹⁵³, J.J. Teoh¹²⁰, F. Tepel¹⁷⁸, S. Terada⁶⁹, K. Terashi¹⁵⁷, J. Terron⁸⁵, S. Terzo¹³,
 M. Testa⁵⁰, R.J. Teuscher^{161,n}, T. Theveneaux-Pelzer⁸⁸, J.P. Thomas¹⁹, J. Thomas-Wilsker⁸⁰,
 P.D. Thompson¹⁹, A.S. Thompson⁵⁶, L.A. Thomsen¹⁷⁹, E. Thomson¹²⁴, M.J. Tibbetts¹⁶,
 R.E. Ticse Torres⁸⁸, V.O. Tikhomirov^{98,ap}, Yu.A. Tikhonov^{111,c}, S. Timoshenko¹⁰⁰, P. Tipton¹⁷⁹,
 S. Tisserant⁸⁸, K. Todome¹⁵⁹, S. Todorova-Nova⁵, J. Tojo⁷³, S. Tokár^{146a}, K. Tokushuku⁶⁹, E. Tolley⁵⁹,
 L. Tomlinson⁸⁷, M. Tomoto¹⁰⁵, L. Tompkins^{145,ag}, K. Toms¹⁰⁷, B. Tong⁵⁹, P. Tornambe⁵¹,
 E. Torrence¹¹⁸, H. Torres¹⁴⁴, E. Torró Pastor¹⁴⁰, J. Toth^{88,ar}, F. Touchard⁸⁸, D.R. Tovey¹⁴¹,
 C.J. Treado¹¹², T. Trefzger¹⁷⁷, A. Tricolí²⁷, I.M. Trigger^{163a}, S. Trincaz-Duvold⁸³, M.F. Tripiana¹³,
 W. Trischuk¹⁶¹, B. Trocmé⁵⁸, A. Trofymov⁴⁵, C. Troncon^{94a}, M. Trottier-McDonald¹⁶, M. Trovatelli¹⁷²,
 L. Truong^{167a,167c}, M. Trzebinski⁴², A. Trzupek⁴², K.W. Tsang^{62a}, J.C-L. Tseng¹²², P.V. Tsiareshka⁹⁵,
 G. Tsipolitis¹⁰, N. Tsirintanis⁹, S. Tsiskaridze¹³, V. Tsiskaridze⁵¹, E.G. Tskhadadze^{54a}, K.M. Tsui^{62a},
 I.I. Tsukerman⁹⁹, V. Tsulaia¹⁶, S. Tsuno⁶⁹, D. Tsybychev¹⁵⁰, Y. Tu^{62b}, A. Tudorache^{28b},
 V. Tudorache^{28b}, T.T. Tulbure^{28a}, A.N. Tuna⁵⁹, S.A. Tupputi^{22a,22b}, S. Turchikhin⁶⁸, D. Turgeman¹⁷⁵,
 I. Turk Cakir^{4b,as}, R. Turra^{94a,94b}, P.M. Tuts³⁸, G. Ucchielli^{22a,22b}, I. Ueda⁶⁹, M. Ughetto^{148a,148b},
 F. Ukegawa¹⁶⁴, G. Unal³², A. Undrus²⁷, G. Unel¹⁶⁶, F.C. Ungaro⁹¹, Y. Unno⁶⁹, C. Unverdorben¹⁰²,
 J. Urban^{146b}, P. Urquijo⁹¹, P. Urrejola⁸⁶, G. Usai⁸, J. Usui⁶⁹, L. Vacavant⁸⁸, V. Vacek¹³⁰, B. Vachon⁹⁰,
 C. Valderanis¹⁰², E. Valdes Santurio^{148a,148b}, N. Valencic¹⁰⁹, S. Valentini^{22a,22b}, A. Valero¹⁷⁰,
 L. Valery¹³, S. Valkar¹³¹, A. Vallier⁵, J.A. Valls Ferrer¹⁷⁰, W. Van Den Wollenberg¹⁰⁹,
 H. van der Graaf¹⁰⁹, N. van Eldik¹⁵⁴, P. van Gemmeren⁶, J. Van Nieuwkoop¹⁴⁴, I. van Vulpen¹⁰⁹,
 M.C. van Woerden¹⁰⁹, M. Vanadia^{134a,134b}, W. Vandelli³², R. Vanguri¹²⁴, A. Vaniachine¹⁶⁰, P. Vankov¹⁰⁹,

G. Vardanyan¹⁸⁰, R. Vari^{134a}, E.W. Varnes⁷, C. Varni^{53a,53b}, T. Varol⁴³, D. Varouchas⁸³, A. Vartapetian⁸, K.E. Varvell¹⁵², J.G. Vasquez¹⁷⁹, G.A. Vasquez^{34b}, F. Vazeille³⁷, T. Vazquez Schroeder⁹⁰, J. Veatch⁵⁷, V. Veeraraghavan⁷, L.M. Veloce¹⁶¹, F. Veloso^{128a,128c}, S. Veneziano^{134a}, A. Ventura^{76a,76b}, M. Venturi¹⁷², N. Venturi¹⁶¹, A. Venturini²⁵, V. Vercesi^{123a}, M. Verducci^{136a,136b}, W. Verkerke¹⁰⁹, J.C. Vermeulen¹⁰⁹, M.C. Vetterli^{144,d}, N. Viaux Maira^{34a}, O. Viazlo⁸⁴, I. Vichou^{169,*}, T. Vickey¹⁴¹, O.E. Vickey Boeriu¹⁴¹, G.H.A. Viehhäuser¹²², S. Viel¹⁶, L. Vigani¹²², M. Villa^{22a,22b}, M. Villaplana Perez^{94a,94b}, E. Vilucchi⁵⁰, M.G. Vincter³¹, V.B. Vinogradov⁶⁸, A. Vishwakarma⁴⁵, C. Vittori^{22a,22b}, I. Vivarelli¹⁵¹, S. Vlachos¹⁰, M. Vlasak¹³⁰, M. Vogel¹⁷⁸, P. Vokac¹³⁰, G. Volpi^{126a,126b}, M. Volpi⁹¹, H. von der Schmitt¹⁰³, E. von Toerne²³, V. Vorobel¹³¹, K. Vorobev¹⁰⁰, M. Vos¹⁷⁰, R. Voss³², J.H. Vossebeld⁷⁷, M. Vozak¹²⁹, N. Vranjes¹⁴, M. Vranjes Milosavljevic¹⁴, V. Vrba¹³⁰, M. Vreeswijk¹⁰⁹, R. Vuillermet³², I. Vukotic³³, P. Wagner²³, W. Wagner¹⁷⁸, H. Wahlberg⁷⁴, S. Wahrmund⁴⁷, J. Wakabayashi¹⁰⁵, J. Walder⁷⁵, R. Walker¹⁰², W. Walkowiak¹⁴³, V. Wallangen^{148a,148b}, C. Wang^{35b}, C. Wang^{36b,at}, F. Wang¹⁷⁶, H. Wang¹⁶, H. Wang³, J. Wang⁴⁵, J. Wang¹⁵², Q. Wang¹¹⁵, R. Wang⁶, S.M. Wang¹⁵³, T. Wang³⁸, W. Wang^{153,au}, W. Wang^{36a}, C. Wanotayaroj¹¹⁸, A. Warburton⁹⁰, C.P. Ward³⁰, D.R. Wardrope⁸¹, A. Washbrook⁴⁹, P.M. Watkins¹⁹, A.T. Watson¹⁹, M.F. Watson¹⁹, G. Watts¹⁴⁰, S. Watts⁸⁷, B.M. Waugh⁸¹, A.F. Webb¹¹, S. Webb⁸⁶, M.S. Weber¹⁸, S.W. Weber¹⁷⁷, S.A. Weber³¹, J.S. Webster⁶, A.R. Weidberg¹²², B. Weinert⁶⁴, J. Weingarten⁵⁷, C. Weiser⁵¹, H. Weits¹⁰⁹, P.S. Wells³², T. Wenaus²⁷, T. Wengler³², S. Wenig³², N. Wermes²³, M.D. Werner⁶⁷, P. Werner³², M. Wessels^{60a}, K. Whalen¹¹⁸, N.L. Whallon¹⁴⁰, A.M. Wharton⁷⁵, A. White⁸, M.J. White¹, R. White^{34b}, D. Whiteson¹⁶⁶, F.J. Wickens¹³³, W. Wiedenmann¹⁷⁶, M. Wielers¹³³, C. Wiglesworth³⁹, L.A.M. Wiik-Fuchs²³, A. Wildauer¹⁰³, F. Wilk⁸⁷, H.G. Wilkens³², H.H. Williams¹²⁴, S. Williams¹⁰⁹, C. Willis⁹³, S. Willocq⁸⁹, J.A. Wilson¹⁹, I. Wingerter-Seez⁵, F. Winklmeier¹¹⁸, O.J. Winston¹⁵¹, B.T. Winter²³, M. Wittgen¹⁴⁵, M. Wobisch^{82,s}, T.M.H. Wolf¹⁰⁹, R. Wolff⁸⁸, M.W. Wolter⁴², H. Wolters^{128a,128c}, S.D. Worm¹³³, B.K. Wosiek⁴², J. Wotschack³², M.J. Woudstra⁸⁷, K.W. Wozniak⁴², M. Wu³³, S.L. Wu¹⁷⁶, X. Wu⁵², Y. Wu⁹², T.R. Wyatt⁸⁷, B.M. Wynne⁴⁹, S. Xella³⁹, Z. Xi⁹², L. Xia^{35c}, D. Xu^{35a}, L. Xu²⁷, B. Yabsley¹⁵², S. Yacoob^{147a}, D. Yamaguchi¹⁵⁹, Y. Yamaguchi¹²⁰, A. Yamamoto⁶⁹, S. Yamamoto¹⁵⁷, T. Yamanaka¹⁵⁷, K. Yamauchi¹⁰⁵, Y. Yamazaki⁷⁰, Z. Yan²⁴, H. Yang^{36c}, H. Yang¹⁶, Y. Yang¹⁵³, Z. Yang¹⁵, W-M. Yao¹⁶, Y.C. Yap⁸³, Y. Yasu⁶⁹, E. Yatsenko⁵, K.H. Yau Wong²³, J. Ye⁴³, S. Ye²⁷, I. Yeletskikh⁶⁸, E. Yildirim⁸⁶, K. Yorita¹⁷⁴, K. Yoshihara¹²⁴, C. Young¹⁴⁵, C.J.S. Young³², S. Youssef²⁴, D.R. Yu¹⁶, J. Yu⁸, J. Yu⁶⁷, L. Yuan⁷⁰, S.P.Y. Yuen²³, I. Yusuff^{30,av}, B. Zabinski⁴², G. Zacharis¹⁰, R. Zaidan¹³, A.M. Zaitsev^{132,ah}, N. Zakharchuk⁴⁵, J. Zalieckas¹⁵, A. Zaman¹⁵⁰, S. Zambito⁵⁹, D. Zanzi⁹¹, C. Zeitnitz¹⁷⁸, M. Zeman¹³⁰, A. Zemla^{41a}, J.C. Zeng¹⁶⁹, Q. Zeng¹⁴⁵, O. Zenin¹³², T. Ženiš^{146a}, D. Zerwas¹¹⁹, D. Zhang⁹², F. Zhang¹⁷⁶, G. Zhang^{36a,ao}, H. Zhang^{35b}, J. Zhang⁶, L. Zhang⁵¹, L. Zhang^{36a}, M. Zhang¹⁶⁹, R. Zhang²³, R. Zhang^{36a,at}, X. Zhang^{36b}, Y. Zhang^{35a}, Z. Zhang¹¹⁹, X. Zhao⁴³, Y. Zhao^{36b,au}, Z. Zhao^{36a}, A. Zhemchugov⁶⁸, J. Zhong¹²², B. Zhou⁹², C. Zhou¹⁷⁶, L. Zhou⁴³, M. Zhou^{35a}, M. Zhou¹⁵⁰, N. Zhou^{35c}, C.G. Zhu^{36b}, H. Zhu^{35a}, J. Zhu⁹², Y. Zhu^{36a}, X. Zhuang^{35a}, K. Zhukov⁹⁸, A. Zibell¹⁷⁷, D. Ziemska⁶⁴, N.I. Zimine⁶⁸, C. Zimmermann⁸⁶, S. Zimmermann⁵¹, Z. Zinonos¹⁰³, M. Zinser⁸⁶, M. Ziolkowski¹⁴³, L. Živković¹⁴, G. Zobernig¹⁷⁶, A. Zoccoli^{22a,22b}, R. Zou³³, M. zur Nedden¹⁷, L. Zwalski³².

¹ Department of Physics, University of Adelaide, Adelaide, Australia

² Physics Department, SUNY Albany, Albany NY, United States of America

³ Department of Physics, University of Alberta, Edmonton AB, Canada

^{4 (a)} Department of Physics, Ankara University, Ankara; ^(b) Istanbul Aydin University, Istanbul; ^(c)

Division of Physics, TOBB University of Economics and Technology, Ankara, Turkey

⁵ LAPP, CNRS/IN2P3 and Université Savoie Mont Blanc, Annecy-le-Vieux, France

⁶ High Energy Physics Division, Argonne National Laboratory, Argonne IL, United States of America

⁷ Department of Physics, University of Arizona, Tucson AZ, United States of America

- ⁸ Department of Physics, The University of Texas at Arlington, Arlington TX, United States of America
⁹ Physics Department, National and Kapodistrian University of Athens, Athens, Greece
¹⁰ Physics Department, National Technical University of Athens, Zografou, Greece
¹¹ Department of Physics, The University of Texas at Austin, Austin TX, United States of America
¹² Institute of Physics, Azerbaijan Academy of Sciences, Baku, Azerbaijan
¹³ Institut de Física d'Altes Energies (IFAE), The Barcelona Institute of Science and Technology, Barcelona, Spain
¹⁴ Institute of Physics, University of Belgrade, Belgrade, Serbia
¹⁵ Department for Physics and Technology, University of Bergen, Bergen, Norway
¹⁶ Physics Division, Lawrence Berkeley National Laboratory and University of California, Berkeley CA, United States of America
¹⁷ Department of Physics, Humboldt University, Berlin, Germany
¹⁸ Albert Einstein Center for Fundamental Physics and Laboratory for High Energy Physics, University of Bern, Bern, Switzerland
¹⁹ School of Physics and Astronomy, University of Birmingham, Birmingham, United Kingdom
²⁰ ^(a) Department of Physics, Bogazici University, Istanbul; ^(b) Department of Physics Engineering, Gaziantep University, Gaziantep; ^(d) Istanbul Bilgi University, Faculty of Engineering and Natural Sciences, Istanbul, Turkey; ^(e) Bahcesehir University, Faculty of Engineering and Natural Sciences, Istanbul, Turkey, Turkey
²¹ Centro de Investigaciones, Universidad Antonio Narino, Bogota, Colombia
²² ^(a) INFN Sezione di Bologna; ^(b) Dipartimento di Fisica e Astronomia, Università di Bologna, Bologna, Italy
²³ Physikalisches Institut, University of Bonn, Bonn, Germany
²⁴ Department of Physics, Boston University, Boston MA, United States of America
²⁵ Department of Physics, Brandeis University, Waltham MA, United States of America
²⁶ ^(a) Universidade Federal do Rio De Janeiro COPPE/EE/IF, Rio de Janeiro; ^(b) Electrical Circuits Department, Federal University of Juiz de Fora (UFJF), Juiz de Fora; ^(c) Federal University of Sao Joao del Rei (UFSJ), Sao Joao del Rei; ^(d) Instituto de Fisica, Universidade de Sao Paulo, Sao Paulo, Brazil
²⁷ Physics Department, Brookhaven National Laboratory, Upton NY, United States of America
²⁸ ^(a) Transilvania University of Brasov, Brasov, Romania; ^(b) Horia Hulubei National Institute of Physics and Nuclear Engineering, Bucharest; ^(c) Department of Physics, Alexandru Ioan Cuza University of Iasi, Iasi, Romania; ^(d) National Institute for Research and Development of Isotopic and Molecular Technologies, Physics Department, Cluj Napoca; ^(e) University Politehnica Bucharest, Bucharest; ^(f) West University in Timisoara, Timisoara, Romania
²⁹ Departamento de Física, Universidad de Buenos Aires, Buenos Aires, Argentina
³⁰ Cavendish Laboratory, University of Cambridge, Cambridge, United Kingdom
³¹ Department of Physics, Carleton University, Ottawa ON, Canada
³² CERN, Geneva, Switzerland
³³ Enrico Fermi Institute, University of Chicago, Chicago IL, United States of America
³⁴ ^(a) Departamento de Física, Pontificia Universidad Católica de Chile, Santiago; ^(b) Departamento de Física, Universidad Técnica Federico Santa María, Valparaíso, Chile
³⁵ ^(a) Institute of High Energy Physics, Chinese Academy of Sciences, Beijing; ^(b) Department of Physics, Nanjing University, Jiangsu; ^(c) Physics Department, Tsinghua University, Beijing 100084, China
³⁶ ^(a) Department of Modern Physics, University of Science and Technology of China, Anhui; ^(b) School of Physics, Shandong University, Shandong; ^(c) Department of Physics and Astronomy, Key Laboratory for Particle Physics, Astrophysics and Cosmology, Ministry of Education; Shanghai Key Laboratory for

- Particle Physics and Cosmology (SKLPPC), Shanghai Jiao Tong University, Shanghai, China
- ³⁷ Laboratoire de Physique Corpusculaire, Université Clermont Auvergne, Université Blaise Pascal, CNRS/IN2P3, Clermont-Ferrand, France
- ³⁸ Nevis Laboratory, Columbia University, Irvington NY, United States of America
- ³⁹ Niels Bohr Institute, University of Copenhagen, Kobenhavn, Denmark
- ⁴⁰ ^(a) INFN Gruppo Collegato di Cosenza, Laboratori Nazionali di Frascati; ^(b) Dipartimento di Fisica, Università della Calabria, Rende, Italy
- ⁴¹ ^(a) AGH University of Science and Technology, Faculty of Physics and Applied Computer Science, Krakow; ^(b) Marian Smoluchowski Institute of Physics, Jagiellonian University, Krakow, Poland
- ⁴² Institute of Nuclear Physics Polish Academy of Sciences, Krakow, Poland
- ⁴³ Physics Department, Southern Methodist University, Dallas TX, United States of America
- ⁴⁴ Physics Department, University of Texas at Dallas, Richardson TX, United States of America
- ⁴⁵ DESY, Hamburg and Zeuthen, Germany
- ⁴⁶ Lehrstuhl für Experimentelle Physik IV, Technische Universität Dortmund, Dortmund, Germany
- ⁴⁷ Institut für Kern- und Teilchenphysik, Technische Universität Dresden, Dresden, Germany
- ⁴⁸ Department of Physics, Duke University, Durham NC, United States of America
- ⁴⁹ SUPA - School of Physics and Astronomy, University of Edinburgh, Edinburgh, United Kingdom
- ⁵⁰ INFN Laboratori Nazionali di Frascati, Frascati, Italy
- ⁵¹ Fakultät für Mathematik und Physik, Albert-Ludwigs-Universität, Freiburg, Germany
- ⁵² Departement de Physique Nucleaire et Corpusculaire, Université de Genève, Geneva, Switzerland
- ⁵³ ^(a) INFN Sezione di Genova; ^(b) Dipartimento di Fisica, Università di Genova, Genova, Italy
- ⁵⁴ ^(a) E. Andronikashvili Institute of Physics, Iv. Javakhishvili Tbilisi State University, Tbilisi; ^(b) High Energy Physics Institute, Tbilisi State University, Tbilisi, Georgia
- ⁵⁵ II Physikalisches Institut, Justus-Liebig-Universität Giessen, Giessen, Germany
- ⁵⁶ SUPA - School of Physics and Astronomy, University of Glasgow, Glasgow, United Kingdom
- ⁵⁷ II Physikalisches Institut, Georg-August-Universität, Göttingen, Germany
- ⁵⁸ Laboratoire de Physique Subatomique et de Cosmologie, Université Grenoble-Alpes, CNRS/IN2P3, Grenoble, France
- ⁵⁹ Laboratory for Particle Physics and Cosmology, Harvard University, Cambridge MA, United States of America
- ⁶⁰ ^(a) Kirchhoff-Institut für Physik, Ruprecht-Karls-Universität Heidelberg, Heidelberg; ^(b) Physikalisches Institut, Ruprecht-Karls-Universität Heidelberg, Heidelberg; ^(c) ZITI Institut für technische Informatik, Ruprecht-Karls-Universität Heidelberg, Mannheim, Germany
- ⁶¹ Faculty of Applied Information Science, Hiroshima Institute of Technology, Hiroshima, Japan
- ⁶² ^(a) Department of Physics, The Chinese University of Hong Kong, Shatin, N.T., Hong Kong; ^(b) Department of Physics, The University of Hong Kong, Hong Kong; ^(c) Department of Physics and Institute for Advanced Study, The Hong Kong University of Science and Technology, Clear Water Bay, Kowloon, Hong Kong, China
- ⁶³ Department of Physics, National Tsing Hua University, Taiwan, Taiwan
- ⁶⁴ Department of Physics, Indiana University, Bloomington IN, United States of America
- ⁶⁵ Institut für Astro- und Teilchenphysik, Leopold-Franzens-Universität, Innsbruck, Austria
- ⁶⁶ University of Iowa, Iowa City IA, United States of America
- ⁶⁷ Department of Physics and Astronomy, Iowa State University, Ames IA, United States of America
- ⁶⁸ Joint Institute for Nuclear Research, JINR Dubna, Dubna, Russia
- ⁶⁹ KEK, High Energy Accelerator Research Organization, Tsukuba, Japan
- ⁷⁰ Graduate School of Science, Kobe University, Kobe, Japan
- ⁷¹ Faculty of Science, Kyoto University, Kyoto, Japan

- ⁷² Kyoto University of Education, Kyoto, Japan
⁷³ Department of Physics, Kyushu University, Fukuoka, Japan
⁷⁴ Instituto de Física La Plata, Universidad Nacional de La Plata and CONICET, La Plata, Argentina
⁷⁵ Physics Department, Lancaster University, Lancaster, United Kingdom
⁷⁶ ^(a) INFN Sezione di Lecce; ^(b) Dipartimento di Matematica e Fisica, Università del Salento, Lecce, Italy
⁷⁷ Oliver Lodge Laboratory, University of Liverpool, Liverpool, United Kingdom
⁷⁸ Department of Experimental Particle Physics, Jožef Stefan Institute and Department of Physics, University of Ljubljana, Ljubljana, Slovenia
⁷⁹ School of Physics and Astronomy, Queen Mary University of London, London, United Kingdom
⁸⁰ Department of Physics, Royal Holloway University of London, Surrey, United Kingdom
⁸¹ Department of Physics and Astronomy, University College London, London, United Kingdom
⁸² Louisiana Tech University, Ruston LA, United States of America
⁸³ Laboratoire de Physique Nucléaire et de Hautes Energies, UPMC and Université Paris-Diderot and CNRS/IN2P3, Paris, France
⁸⁴ Fysiska institutionen, Lunds universitet, Lund, Sweden
⁸⁵ Departamento de Fisica Teorica C-15, Universidad Autonoma de Madrid, Madrid, Spain
⁸⁶ Institut für Physik, Universität Mainz, Mainz, Germany
⁸⁷ School of Physics and Astronomy, University of Manchester, Manchester, United Kingdom
⁸⁸ CPPM, Aix-Marseille Université and CNRS/IN2P3, Marseille, France
⁸⁹ Department of Physics, University of Massachusetts, Amherst MA, United States of America
⁹⁰ Department of Physics, McGill University, Montreal QC, Canada
⁹¹ School of Physics, University of Melbourne, Victoria, Australia
⁹² Department of Physics, The University of Michigan, Ann Arbor MI, United States of America
⁹³ Department of Physics and Astronomy, Michigan State University, East Lansing MI, United States of America
⁹⁴ ^(a) INFN Sezione di Milano; ^(b) Dipartimento di Fisica, Università di Milano, Milano, Italy
⁹⁵ B.I. Stepanov Institute of Physics, National Academy of Sciences of Belarus, Minsk, Republic of Belarus
⁹⁶ Research Institute for Nuclear Problems of Byelorussian State University, Minsk, Republic of Belarus
⁹⁷ Group of Particle Physics, University of Montreal, Montreal QC, Canada
⁹⁸ P.N. Lebedev Physical Institute of the Russian Academy of Sciences, Moscow, Russia
⁹⁹ Institute for Theoretical and Experimental Physics (ITEP), Moscow, Russia
¹⁰⁰ National Research Nuclear University MEPhI, Moscow, Russia
¹⁰¹ D.V. Skobeltsyn Institute of Nuclear Physics, M.V. Lomonosov Moscow State University, Moscow, Russia
¹⁰² Fakultät für Physik, Ludwig-Maximilians-Universität München, München, Germany
¹⁰³ Max-Planck-Institut für Physik (Werner-Heisenberg-Institut), München, Germany
¹⁰⁴ Nagasaki Institute of Applied Science, Nagasaki, Japan
¹⁰⁵ Graduate School of Science and Kobayashi-Maskawa Institute, Nagoya University, Nagoya, Japan
¹⁰⁶ ^(a) INFN Sezione di Napoli; ^(b) Dipartimento di Fisica, Università di Napoli, Napoli, Italy
¹⁰⁷ Department of Physics and Astronomy, University of New Mexico, Albuquerque NM, United States of America
¹⁰⁸ Institute for Mathematics, Astrophysics and Particle Physics, Radboud University Nijmegen/Nikhef, Nijmegen, Netherlands
¹⁰⁹ Nikhef National Institute for Subatomic Physics and University of Amsterdam, Amsterdam, Netherlands

- ¹¹⁰ Department of Physics, Northern Illinois University, DeKalb IL, United States of America
¹¹¹ Budker Institute of Nuclear Physics, SB RAS, Novosibirsk, Russia
¹¹² Department of Physics, New York University, New York NY, United States of America
¹¹³ Ohio State University, Columbus OH, United States of America
¹¹⁴ Faculty of Science, Okayama University, Okayama, Japan
¹¹⁵ Homer L. Dodge Department of Physics and Astronomy, University of Oklahoma, Norman OK, United States of America
¹¹⁶ Department of Physics, Oklahoma State University, Stillwater OK, United States of America
¹¹⁷ Palacký University, RCPTM, Olomouc, Czech Republic
¹¹⁸ Center for High Energy Physics, University of Oregon, Eugene OR, United States of America
¹¹⁹ LAL, Univ. Paris-Sud, CNRS/IN2P3, Université Paris-Saclay, Orsay, France
¹²⁰ Graduate School of Science, Osaka University, Osaka, Japan
¹²¹ Department of Physics, University of Oslo, Oslo, Norway
¹²² Department of Physics, Oxford University, Oxford, United Kingdom
¹²³ ^(a) INFN Sezione di Pavia; ^(b) Dipartimento di Fisica, Università di Pavia, Pavia, Italy
¹²⁴ Department of Physics, University of Pennsylvania, Philadelphia PA, United States of America
¹²⁵ National Research Centre "Kurchatov Institute" B.P.Konstantinov Petersburg Nuclear Physics Institute, St. Petersburg, Russia
¹²⁶ ^(a) INFN Sezione di Pisa; ^(b) Dipartimento di Fisica E. Fermi, Università di Pisa, Pisa, Italy
¹²⁷ Department of Physics and Astronomy, University of Pittsburgh, Pittsburgh PA, United States of America
¹²⁸ ^(a) Laboratório de Instrumentação e Física Experimental de Partículas - LIP, Lisboa; ^(b) Faculdade de Ciências, Universidade de Lisboa, Lisboa; ^(c) Department of Physics, University of Coimbra, Coimbra; ^(d) Centro de Física Nuclear da Universidade de Lisboa, Lisboa; ^(e) Departamento de Física, Universidade do Minho, Braga; ^(f) Departamento de Física Teórica y del Cosmos and CAFPE, Universidad de Granada, Granada (Spain); ^(g) Dep Física and CEFITEC of Faculdade de Ciencias e Tecnologia, Universidade Nova de Lisboa, Caparica, Portugal
¹²⁹ Institute of Physics, Academy of Sciences of the Czech Republic, Praha, Czech Republic
¹³⁰ Czech Technical University in Prague, Praha, Czech Republic
¹³¹ Charles University, Faculty of Mathematics and Physics, Prague, Czech Republic
¹³² State Research Center Institute for High Energy Physics (Protvino), NRC KI, Russia
¹³³ Particle Physics Department, Rutherford Appleton Laboratory, Didcot, United Kingdom
¹³⁴ ^(a) INFN Sezione di Roma; ^(b) Dipartimento di Fisica, Sapienza Università di Roma, Roma, Italy
¹³⁵ ^(a) INFN Sezione di Roma Tor Vergata; ^(b) Dipartimento di Fisica, Università di Roma Tor Vergata, Roma, Italy
¹³⁶ ^(a) INFN Sezione di Roma Tre; ^(b) Dipartimento di Matematica e Fisica, Università Roma Tre, Roma, Italy
¹³⁷ ^(a) Faculté des Sciences Ain Chock, Réseau Universitaire de Physique des Hautes Energies - Université Hassan II, Casablanca; ^(b) Centre National de l'Energie des Sciences Techniques Nucléaires, Rabat; ^(c) Faculté des Sciences Semlalia, Université Cadi Ayyad, LPHEA-Marrakech; ^(d) Faculté des Sciences, Université Mohamed Premier and LPTPM, Oujda; ^(e) Faculté des sciences, Université Mohammed V, Rabat, Morocco
¹³⁸ DSM/IRFU (Institut de Recherches sur les Lois Fondamentales de l'Univers), CEA Saclay (Commissariat à l'Energie Atomique et aux Energies Alternatives), Gif-sur-Yvette, France
¹³⁹ Santa Cruz Institute for Particle Physics, University of California Santa Cruz, Santa Cruz CA, United States of America
¹⁴⁰ Department of Physics, University of Washington, Seattle WA, United States of America

- ¹⁴¹ Department of Physics and Astronomy, University of Sheffield, Sheffield, United Kingdom
¹⁴² Department of Physics, Shinshu University, Nagano, Japan
¹⁴³ Fachbereich Physik, Universität Siegen, Siegen, Germany
¹⁴⁴ Department of Physics, Simon Fraser University, Burnaby BC, Canada
¹⁴⁵ SLAC National Accelerator Laboratory, Stanford CA, United States of America
¹⁴⁶ ^(a) Faculty of Mathematics, Physics & Informatics, Comenius University, Bratislava; ^(b) Department of Subnuclear Physics, Institute of Experimental Physics of the Slovak Academy of Sciences, Kosice, Slovak Republic
¹⁴⁷ ^(a) Department of Physics, University of Cape Town, Cape Town; ^(b) Department of Physics, University of Johannesburg, Johannesburg; ^(c) School of Physics, University of the Witwatersrand, Johannesburg, South Africa
¹⁴⁸ ^(a) Department of Physics, Stockholm University; ^(b) The Oskar Klein Centre, Stockholm, Sweden
¹⁴⁹ Physics Department, Royal Institute of Technology, Stockholm, Sweden
¹⁵⁰ Departments of Physics & Astronomy and Chemistry, Stony Brook University, Stony Brook NY, United States of America
¹⁵¹ Department of Physics and Astronomy, University of Sussex, Brighton, United Kingdom
¹⁵² School of Physics, University of Sydney, Sydney, Australia
¹⁵³ Institute of Physics, Academia Sinica, Taipei, Taiwan
¹⁵⁴ Department of Physics, Technion: Israel Institute of Technology, Haifa, Israel
¹⁵⁵ Raymond and Beverly Sackler School of Physics and Astronomy, Tel Aviv University, Tel Aviv, Israel
¹⁵⁶ Department of Physics, Aristotle University of Thessaloniki, Thessaloniki, Greece
¹⁵⁷ International Center for Elementary Particle Physics and Department of Physics, The University of Tokyo, Tokyo, Japan
¹⁵⁸ Graduate School of Science and Technology, Tokyo Metropolitan University, Tokyo, Japan
¹⁵⁹ Department of Physics, Tokyo Institute of Technology, Tokyo, Japan
¹⁶⁰ Tomsk State University, Tomsk, Russia, Russia
¹⁶¹ Department of Physics, University of Toronto, Toronto ON, Canada
¹⁶² ^(a) INFN-TIFPA; ^(b) University of Trento, Trento, Italy, Italy
¹⁶³ ^(a) TRIUMF, Vancouver BC; ^(b) Department of Physics and Astronomy, York University, Toronto ON, Canada
¹⁶⁴ Faculty of Pure and Applied Sciences, and Center for Integrated Research in Fundamental Science and Engineering, University of Tsukuba, Tsukuba, Japan
¹⁶⁵ Department of Physics and Astronomy, Tufts University, Medford MA, United States of America
¹⁶⁶ Department of Physics and Astronomy, University of California Irvine, Irvine CA, United States of America
¹⁶⁷ ^(a) INFN Gruppo Collegato di Udine, Sezione di Trieste, Udine; ^(b) ICTP, Trieste; ^(c) Dipartimento di Chimica, Fisica e Ambiente, Università di Udine, Udine, Italy
¹⁶⁸ Department of Physics and Astronomy, University of Uppsala, Uppsala, Sweden
¹⁶⁹ Department of Physics, University of Illinois, Urbana IL, United States of America
¹⁷⁰ Instituto de Fisica Corpuscular (IFIC) and Departamento de Fisica Atomica, Molecular y Nuclear and Departamento de Ingeniería Electrónica and Instituto de Microelectrónica de Barcelona (IMB-CNM), University of Valencia and CSIC, Valencia, Spain
¹⁷¹ Department of Physics, University of British Columbia, Vancouver BC, Canada
¹⁷² Department of Physics and Astronomy, University of Victoria, Victoria BC, Canada
¹⁷³ Department of Physics, University of Warwick, Coventry, United Kingdom
¹⁷⁴ Waseda University, Tokyo, Japan

- ¹⁷⁵ Department of Particle Physics, The Weizmann Institute of Science, Rehovot, Israel
¹⁷⁶ Department of Physics, University of Wisconsin, Madison WI, United States of America
¹⁷⁷ Fakultät für Physik und Astronomie, Julius-Maximilians-Universität, Würzburg, Germany
¹⁷⁸ Fakultät für Mathematik und Naturwissenschaften, Fachgruppe Physik, Bergische Universität Wuppertal, Wuppertal, Germany
¹⁷⁹ Department of Physics, Yale University, New Haven CT, United States of America
¹⁸⁰ Yerevan Physics Institute, Yerevan, Armenia
¹⁸¹ Centre de Calcul de l’Institut National de Physique Nucléaire et de Physique des Particules (IN2P3), Villeurbanne, France
^a Also at Department of Physics, King’s College London, London, United Kingdom
^b Also at Institute of Physics, Azerbaijan Academy of Sciences, Baku, Azerbaijan
^c Also at Novosibirsk State University, Novosibirsk, Russia
^d Also at TRIUMF, Vancouver BC, Canada
^e Also at Department of Physics & Astronomy, University of Louisville, Louisville, KY, United States of America
^f Also at Physics Department, An-Najah National University, Nablus, Palestine
^g Also at Department of Physics, California State University, Fresno CA, United States of America
^h Also at Department of Physics, University of Fribourg, Fribourg, Switzerland
ⁱ Also at Departament de Fisica de la Universitat Autonoma de Barcelona, Barcelona, Spain
^j Also at Departamento de Fisica e Astronomia, Faculdade de Ciencias, Universidade do Porto, Portugal
^k Also at Tomsk State University, Tomsk, Russia, Russia
^l Also at The Collaborative Innovation Center of Quantum Matter (CICQM), Beijing, China
^m Also at Universita di Napoli Parthenope, Napoli, Italy
ⁿ Also at Institute of Particle Physics (IPP), Canada
^o Also at Horia Hulubei National Institute of Physics and Nuclear Engineering, Bucharest, Romania
^p Also at Department of Physics, St. Petersburg State Polytechnical University, St. Petersburg, Russia
^q Also at Department of Physics, The University of Michigan, Ann Arbor MI, United States of America
^r Also at Centre for High Performance Computing, CSIR Campus, Rosebank, Cape Town, South Africa
^s Also at Louisiana Tech University, Ruston LA, United States of America
^t Also at Institutio Catalana de Recerca i Estudis Avancats, ICREA, Barcelona, Spain
^u Also at Graduate School of Science, Osaka University, Osaka, Japan
^v Also at Fakultät für Mathematik und Physik, Albert-Ludwigs-Universität, Freiburg, Germany
^w Also at Institute for Mathematics, Astrophysics and Particle Physics, Radboud University Nijmegen/Nikhef, Nijmegen, Netherlands
^x Also at Department of Physics, The University of Texas at Austin, Austin TX, United States of America
^y Also at Institute of Theoretical Physics, Ilia State University, Tbilisi, Georgia
^z Also at CERN, Geneva, Switzerland
^{aa} Also at Georgian Technical University (GTU), Tbilisi, Georgia
^{ab} Also at Ochadai Academic Production, Ochanomizu University, Tokyo, Japan
^{ac} Also at Manhattan College, New York NY, United States of America
^{ad} Also at Academia Sinica Grid Computing, Institute of Physics, Academia Sinica, Taipei, Taiwan
^{ae} Also at School of Physics, Shandong University, Shandong, China
^{af} Also at Departamento de Física Teórica y del Cosmos and CAFPE, Universidad de Granada, Granada (Spain), Portugal
^{ag} Also at Department of Physics, California State University, Sacramento CA, United States of America
^{ah} Also at Moscow Institute of Physics and Technology State University, Dolgoprudny, Russia

ai Also at Departement de Physique Nucleaire et Corpusculaire, Université de Genève, Geneva, Switzerland

aj Also at International School for Advanced Studies (SISSA), Trieste, Italy

ak Also at Institut de Física d'Altes Energies (IFAE), The Barcelona Institute of Science and Technology, Barcelona, Spain

al Also at School of Physics, Sun Yat-sen University, Guangzhou, China

am Also at Institute for Nuclear Research and Nuclear Energy (INRNE) of the Bulgarian Academy of Sciences, Sofia, Bulgaria

an Also at Faculty of Physics, M.V.Lomonosov Moscow State University, Moscow, Russia

ao Also at Institute of Physics, Academia Sinica, Taipei, Taiwan

ap Also at National Research Nuclear University MEPhI, Moscow, Russia

aq Also at Department of Physics, Stanford University, Stanford CA, United States of America

ar Also at Institute for Particle and Nuclear Physics, Wigner Research Centre for Physics, Budapest, Hungary

as Also at Giresun University, Faculty of Engineering, Turkey

at Also at CPPM, Aix-Marseille Université and CNRS/IN2P3, Marseille, France

au Also at Department of Physics, Nanjing University, Jiangsu, China

av Also at University of Malaya, Department of Physics, Kuala Lumpur, Malaysia

aw Also at LAL, Univ. Paris-Sud, CNRS/IN2P3, Université Paris-Saclay, Orsay, France

* Deceased